Angewandte Chemie
GDCh
Eine Zeitschrift der Gesellschaft Deutscher Chemiker
www.angewandte.de

Akzeptierter Artikel

Titel: Excited State Anions in Organic Transformations

Autoren: Matthias Schmalzbauer, Michela Marcon, and Burkhard König

Zitierweise: *Angew. Chem. Int. Ed.* 10.1002/anie.202009288

Link zur VoR: https://doi.org/10.1002/anie.202009288

WILEY-VCH

10.1002/ange.202009288

WILEY-VCH

Excited State Anions in Organic Transformations

Matthias Schmalzbauer, Michela Marcon and Burkhard König*[a]

Dedicated to Prof. Ilhyong Ryu on the occasion of his 70th birthday

[*] M. Schmalzbauer, M. Marcon, Prof. B. König
Faculty of Chemistry and Pharmacy
University of Regensburg
Universitätsstraße 31, 93053 Regensburg, Germany
E-mail: burkhard.koenig@ur.de

Abstract: Utilizing light is a smart way to fuel chemical transformations as it allows to selectively focus the energy on certain molecules. Many reactions involving electronically excited species proceed *via* open-shell intermediates enabling novel and unique routes to expand the hitherto used synthetic toolbox in organic chemistry. The direct conversion of non-prefunctionalized, less activated compounds is a highly desirable goal to pave the way towards a more sustainable and atom-economic chemistry. Photoexcited closed-shell anions have been shown to reach extreme potentials in single electron transfer reactions and reveal unusual excited state reactivity. It is therefore surprising, that their use as reagent or as photocatalyst is limited to a few examples. In this review, we briefly discuss the characteristics of anionic photochemistry, highlight pioneering work and show recent progress which has been made by utilizing photoexcited anionic species in organic synthesis.

1. Introduction

Initial attention to the versatile reaction modes of photoexcited organic anions and their special spectroscopic behaviour was drawn by the early reviews of Fox[1] and Tolbert[2]. Since then, other excellent publications followed, summarizing the photochemistry of excited organic anions with focus on their photoreductive properties and underlining the peculiarities of anionic organic molecules in photochemistry.[3,4] Compared to the neutral species, the absorption of an organic anion is usually red-shifted, which facilitates the selective excitation in complex mixtures and often allows to use visible light. Along with the enhanced electron-electron repulsion found in anionic molecules, negatively charged species are expected to act as particularly potent electron donors from their photoexcited states. In addition, a single electron transfer from an anionic donor to a neutral acceptor gives rise to a neutral radical and a radical anion. These species are free of attracting forces and are able to diffuse freely, which suppresses back electron transfer (BET) reactions resulting in higher reaction efficiencies. Organic anions can be easily formed in presence of base and their rather long excited state lifetimes distinguish them from radical anions.

Excited anionic species are also utilized in key photochemical steps in biology. For instance, in an ATP-driven process, the excited oxyluciferin anion causes the bioluminescence of fireflies.[5] Moreover, phototrophic organisms show locomotory movement upon stimulus of light. The photoactive yellow protein (PYP) encloses the anionic *trans-para*-coumaric acid as blue-light photoreceptor. Subsequent *trans-cis* isomerization of the excited chromophore induces a conformational change of the protein leading to a biological signal transduction.[6] The enzyme-mediated repair of photodamaged DNA is another well-known example dealing with excited anions in living cells. A crucial step is the photoinduced electron transfer from the excited cofactor flavin adenine dinucleotide ($FADH^-$) which provides an electron for the light-driven repair catalyzed by photolyases.[7,8]

Literally, the last decade has been a very exciting time in terms of photochemistry and many novel chemical transformations have been developed which complement the available synthetic toolbox. We are sure that, inspired by nature and the herein presented examples, the photochemistry of closed-shell anions will be further developed towards the generation of ever stronger light-activated reductants and novel reaction modes. In this review, we briefly summarize key spectroscopic and electrochemical properties of organic anions and provide an overview of the versatile photochemistry of anionic species with a special focus on recent examples of organic anions used as photocatalysts or as light-activated reagents.

1.1. Spectroscopic Properties of Organic Anions

The chemistry of molecules excited by light is initiated by the absorption of a photon and thus, we will start with discussing the peculiarities of the absorption spectra for closed-shell anions. Compared to their neutral precursors, organic anions usually experience a significant bathochromic shift in their absorption spectra and pronounced absorption bands can be attributed to π, π^* transitions. The narrowed gap between the highest occupied molecular orbital (HOMO) and the lowest unoccupied molecular orbital (LUMO, see Figure 1) causing the red-shift can be primarily explained by the increased shielding of the core due to an imbalance of charges. The strength of the electric field is reduced and electrons in the HOMO sense much weaker attracting forces. As a result, the spatial distribution of electrons becomes more diffuse as if the conjugation length is extended.[1,9] The absorption of organic anions is also affected by size and nature of the countercation, solvent polarity and ion pairing effects in solution. In non-polar or weakly polar solvents, contact ion pairs are formed and the properties of the anionic species are strongly influenced by the character of the countercation.

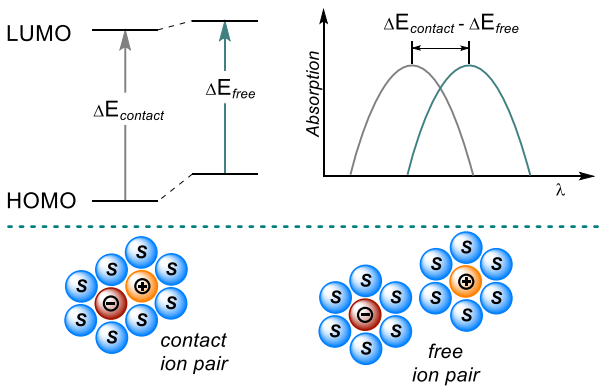

Figure 1. Energetic destabilization of the ground state of a free ion pair in polar solvent compared to the contact ion pair in non-polar solvent and influence on the absorption spectrum.

In contrast, the increased solubility of ions in polar solvents, induced by aligning molecular dipoles, causes solvent-separated

or free ion pairs and the mutual ionic interaction is diminished. In general, an increase in solvent polarity and/or ionic radius of the countercation results in a bathochromic shift of the absorption, which can be attributed to a destabilization of the ground state ion pair. This destabilization effect is less pronounced in the excited state.[1,4]

Similarly, the emission of excited organic anions is usually influenced by solvent polarity and countercation. The fluorescence decay of sodium 2-naphtholate was studied in different solvents.[10] For polar protic and polar aprotic solvents, a mono-exponential fluorescence decay was observed. However, in polar protic MeOH the fluorescence lifetime was remarkably decreased and the emission spectrum was blue-shifted compared to polar aprotic DMF or DMSO, which the authors attribute to a stabilization of the anion ground state caused by strong hydrogen bonding of the solvent. In weakly polar THF contact ion pairs and solvent separated ion pairs of 2-naphtholate and Na^+ coexist and cause a bi-exponential fluorescence decay due to varying fluorescence lifetimes. Upon addition of crown-ether to the system, a mono-exponential decay was recorded suggesting that sodium cations are complexed and the ion pairs formed with naphtholate are solvent separated in nature. Owing to the lack of ground state stabilization in solvent separated or free ion pairs, lifetimes similar to experiments in polar aprotic solvents were found in presence of a crown-ether.

The nature of ion pairing might also affect the efficiency of bimolecular electron transfer processes. Tamaoki and co-workers studied the quantum yield for the photodissociation of a benzene diazonium salt **1** with 9,10-dimethoxyanthracene-2-sulfonate (**2**) being the visible-light-absorbing counteranion (Scheme 1).[11] The photodecomposition of the benzene diazonium cation **1** initiated by PET from the excited anion **2** was found to be six-times higher in $CHCl_3$ compared to MeCN. The difference in reactivity of the diazonium salt between the solvents was explained by the different nature of ion pairs formed. The weakly polar solvent $CHCl_3$ promotes a fast reaction due to the close proximity of **1** and **2** in a tight ion pair. Solvent separated loose ion pairs in polar MeCN allowed to measure a distinct fluorescence lifetime. Upon excitation in polar media the anionic donor needs to initially encounter a cationic acceptor to trigger the photodecomposition and hence increased lifetimes are recorded. For a more comprehensive discussion of ion-pairing and solvent effects, we refer to several excellent reports.[4,10,12–14]

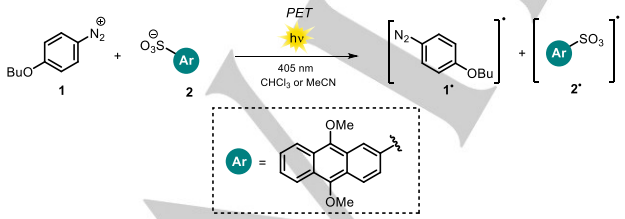

Scheme 1. The rate of photoinduced electron transfer is influenced by the solvent polarity: fast in $CHCl_3$ (tight pair), slow in MeCN (loose pair)

1.2. Photoinduced Electron Transfer

Electron transfer reactions from electronically excited states of molecules are among the earliest photochemical reactions reported.[15] Photoexcited molecules exhibit increased reduction and oxidation potentials compared to their ground state and the resulting excited state potentials can be estimated, according to the free enthalpy change of a PET, by measuring the ground state potentials $E_{1/2}$ and the transition energy $E_{0,0}$ (see Figure 2).[16] In polar organic solvents the electrostatic work term usually contributes little to the free enthalpy change and is frequently omitted.[17]

PET from a neutral excited-state donor (*D) to a neutral ground-state acceptor (A) causes a charge separation, resulting in a pair of radical ions. In contrast, the PET from an anionic excited-state donor to a neutral acceptor can be considered as a charge shift, generating products that are free of electrostatic attraction and expected to diffuse freely (Scheme 2). Hence, the lost channel of a back electron transfer, which would regenerate the initial non-excited *status quo*, is less competitive in a charge-shift process.[18]

Scheme 2. Charge separation with neutral donor (left) and charge shift with anionic donor (right).

An anionic molecule is considered as a superior electron donor compared to its neutral parent. Both repulsion between electrons and the shielding from the nucleus are increased. As a consequence, the excess negative charge facilitates the removal of an electron. Experimentally, this becomes apparent when solvated electrons are expelled from organic anions in a biphotonic process using energy-rich UV light[19] in glassy matrices (77 K) or pulsed high-energy lasers[20,21] in alkaline aqueous solution. Working with visible-light LEDs and in common organic solvents however, renders the photo-ejection of an electron unlikely to occur and hence under these conditions electron transfer reactions are prevailing. We recently demonstrated that 9-anthrone and its derivatives are easily deprotonated in presence of carbonate base to form colored anions (*e.g.* **ANT**$^-$, Figure 2), which upon visible-light excitation turn into remarkably strong reductants.[22] Cyclic voltammetry measurements in alkaline DMSO revealed that the anionic ground state is already a good reductant, as the excess charge is removed easily due to resonance stabilization of the resulting radical. In sharp contrast, the dianions of fluorescein **FL**$^{2-}$ or eosin Y (**EY**$^{2-}$) show a significantly decreased tendency towards electrochemical oxidation in alkaline MeOH and hence, the resulting excited state oxidation potentials are only moderate (*cf.*, Table 1, Entry 5-7).[23]

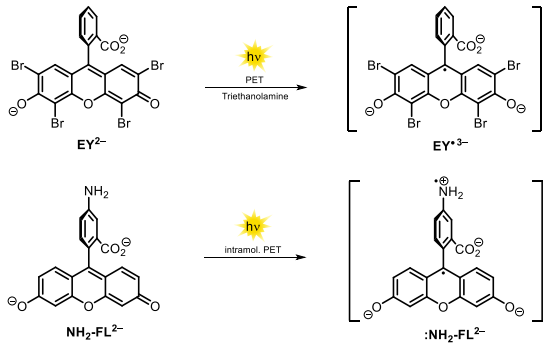

Scheme 3. Formation of the eosin Y radical trianion upon PET in presence of triethanolamine (top). Intramolecular PET from the amino group causing self-quenching of the fluorescence.

Furthermore, it was reported that FL^{2-} and EY^{2-}, although being present as ground state dianions, are easily reduced upon photoexcitation in basic solutions containing triethanolamine or phenol to form radical trianions (Scheme 3, top).[24–28] Walt and co-workers attached an amino group on the benzoate scaffold of fluorescein NH_2-FL^{2-} and found that the fluorescence quantum yield dropped by almost a factor of 60. They explained this observation by an intramolecular PET from the nitrogen lone pair to the fluorescein scaffold (Scheme 3, bottom). A similar fluorescence quantum yield with respect to non-modified FL^{2-} was however recorded when adjusting the pH of the solution to a value around the pK_a of the aromatic amine. Due to protonation of the amine, the nitrogen lone pair is no longer available for intramolecular PET resulting in increased fluorescence.[29] In 1991, Soumillion *et al.* showed that the fluorescence of the excited anion of the xanthene dye resorufin is quenched in presence of 2-naphtholate and the formation of a radical dianion of resorufin was proposed.[18] The moderate reducing abilities of negatively charged xanthene dyes (*e.g.* EY^{2-}, FL^{2-}) can be explained by an overwhelming contribution of the electron-deficient conjugated system to the overall electronic properties. Thus, to obtain strongly reducing excited anions, a facile single electron oxidation is crucial (*cf.*, Table 1, Entry 5-6 show similar values for $E_{0,0}$ but differ significantly in their ground state and excited state oxidation potentials).

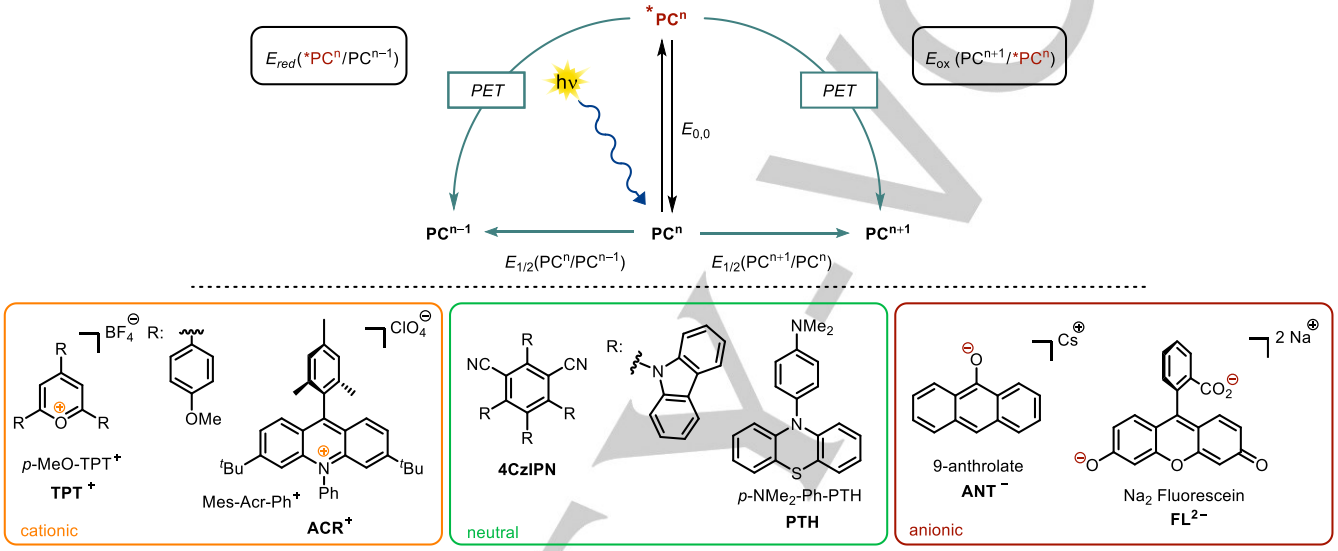

Figure 2. Diagram of ground and excited state potentials of a photocatalyst (PC, top). Representatives of cationic, neutral and anionic organic photocatalyst (bottom).

Table 1. Ground state ($E_{1/2}$) and excited state (E_{red}, E_{ox}) redox potentials of selected cationic, neutral and anionic photocatalysts (PC) and the corresponding transition energies ($E_{0,0}$).

Entry	PC^n	$E_{1/2}(PC^n/PC^{n-1})$	$E_{red}(^*PC^n/PC^{n-1})$	$E_{1/2}(PC^{n+1}/PC^n)$	$E_{ox}(PC^{n+1}/^*PC^n)$	$E_{0,0}$ [eV]
1[17]	**TPT$^+$**	− 0.50[a]	+ 1.84	-	-	2.34[b]
2[30]	**ACR$^+$**	− 0.59[c]	+ 2.08	-	-	2.67
3[31]	**4CzIPN**	− 1.24[d]	+ 1.43	+ 1.49[d]	− 1.18	2.67
4[32]	**PTH**	-	-	+ 0.57[d]	− 2.5	3.1
5[22]	**ANT$^-$**	-	-	− 0.34[d,e]	− 2.65	2.31
6[23]	**FL^{2-}**	-	-	+ 0.87[f]	− 1.55	2.42
7[17]	**EY^{2-}**	− 1.06	+ 1.23[g,h] + 0.83[i,h]	+ 0.76	− 1.58[g,h] − 1.08[i,h]	2.31[g] 1.91[h]
8[71]	**PhPH$^-$**	-	-	- 0.10[e]	− 3.16	3.06
9[78]	**BIA-H.1$^-$**	-	-	+0.06[j]	− 2.71	2.77[k]
10[85]	**TMA$^-$**	-	-	- 0.51[d,e]	− 2.92	2.41

Potentials are reported *vs.* saturated calomel electrode (SCE). Transition energy $E_{0,0}$ was determined from the intersection of normalized absorption and emission spectra. [a]Potential recorded *vs.* normal hydrogen electrode (NHE) and converted to SCE by subtracting 0.141 V; [b]Determined from the highest energy emission maximum; [c]Potential recorded vs. Ag/AgCl and converted to SCE by subtracting 0.03 V; [d]Potential recorded *vs.* the ferrocene redox couple (Fc^+/Fc) and converted to SCE by adding 0.38 V; [e]Potential was measured in dry degassed DMSO with excess of Cs_2CO_3; [f]Potential was measured in MeOH containing NaOH (0.1 mM) against Ag/AgCl and referenced to SCE by conversion; [g]Values for singlet excited state; [h]Potential recorded vs. Ag/AgCl and converted to SCE by subtracting 0.039 V, [i]Values for triplet excited state; [j]Potential was measured in MeCN with excess ^{t}BuOK; [k]Estimated by the end absorption wavelength possessing 0.02 absorbance at 4.0 × 10^{-5} M.

10.1002/ange.202009288

2. Anionic Compounds as Photocatalysts

2.1 Photoredox Catalysis

During the last decade, impressive progress has been made in the field of synthetic photoredox catalysis and many novel transformations, which were previously inaccessible, have been developed. Photoexciting a molecule changes the electron distribution in the molecular orbitals resulting in both increased oxidizing- and reducing abilities of the excited species compared to the ground state (see Figure 2). These redox properties can be fine-tuned by attaching electron donating or withdrawing substituents.[30–32] Up to now, a variety of photocatalysts have been reported which are often classified regarding their composition into polypyridyl transition metal complexes,[33] organic dyes[17] or polyoxometalates[34] (POMs). In addition, heterogenous organic semiconductors were successfully employed as photocatalysts.[35] Their intrinsic photophysical properties like excited state redox potential, absorption of light or the excited state lifetime define the scope and limitations of chemical reactions. Selected examples of organic photocatalysts are depicted in Figure 2. The photochemistry of the non-charged donor-acceptor dyad **4CzIPN** covers a broad electrochemical range (see Table 1, Entry 3). Bearing a versatile excited-state reduction and oxidation potential, it is often used to replace precious and toxic Ru- or Ir-polypyridyl complexes.[31,36] However, to convert less activated substrates *via* photoinduced single electron transfer, the frontiers need to be pushed towards higher excited state potentials. Recently, it was shown that photoexcited, electron-rich N-arylphenothiazines (*e.g.* **PTH**) act as very strong reductants but these compounds do not absorb in the visible range and hence UV-light is necessary which might interfere with other reaction components. Large Stokes shifts were found for the substituted N-arylphenothiazines which result in high transition energy values (*cf.,* Table 1, Entry 4).[32]

Apart from commonly used neutral organic dyes, molecules with a charged or an open-shell ground state or both were found to significantly increase achievable excited state potentials and allowed to widen the substrate scope for photoinduced electron transfer reactions (Scheme 4). Several organic dyes form stable and coloured radical anions in presence of suitable sacrificial donors *via* PET and hence, enable a subsequent second excitation (see Scheme 4, A).[37–40] The versatile photochemistry of excited radical anions allowed to convert various (hetero)aryl halides in coupling reactions and has been subject of several reviews.[41–44] Very recently, this strategy was reported to promote Birch-type reductions of benzene derivatives upon visible-light irradiation.[45] In contrast, the formation of super-oxidants has been reported upon photoexcitation of stable, chemically generated phenothiazine radical cations (see Scheme 4, B).[46] Furthermore, electron transfer from photoexcited doublet states of neutral radicals has been studied.[47–51] The acridine radical **ACR**$^{\bullet}$ was recently found to act as an extremely potent photo-reductant upon excitation with blacklight (see Scheme 4, C).[52] Although enabling high redox potentials, the photochemistry of excited open-shell species suffers from short lifetimes which are usually in the picosecond range.[52–54] As the photochemistry of open-shell molecules is beyond the scope of this review, the interested reader is referred to cited literature.

Photoreactions using catalytic amounts of closed-shell cations were found to be synthetically very useful (Scheme 4, D). The pioneering work of Fukuzumi and co-workers[55] paved the way for plenty of publications using acridinium-based donor-acceptor dyads as strongly oxidizing photocatalysts.[17,56–59] Moreover, a new benchmark regarding the excited state potential was set by using pyrylium-, quinolinium- or diazapyrenium salts as extremely powerful photooxidants.[17] Among other cationic dyes, the photoexcited pyrylium- or acridinium salts (*e.g.* **TPT**$^{+}$ and **ACR**$^{+}$, Figure 2) are strong oxidants in their excited states and found widespread synthetic applications.[17,60–67] Surprisingly, in contrast to the wealth of reports dealing with photoexcited cations, the photochemistry of closed-shell anions received far less attention although it constitutes the logical equivalent (Scheme 4, E).

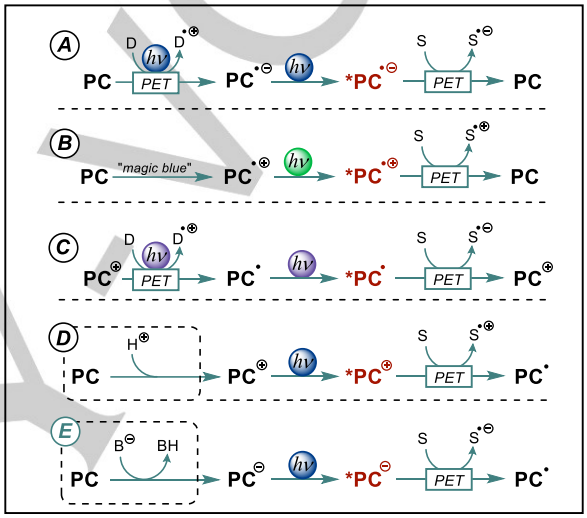

Scheme 4. Approaches leading to reactive excited state photocatalysts with extreme redox potentials (red) allowing to convert non-activated substrates (S); The initial activation by protonation/deprotonation (see D, E) is not required when the salt of the catalyst is directly used.

Hence, in the following section the ability of anionic photocatalysts to drive challenging transformations is underlined based on selected examples. Due to their moderate redox-potentials and the wealth of available reviews, reactions of anionic xanthene dyes like eosin Y, rose bengal or fluorescein are not discussed herein.[17,68–70] Furthermore, examples where anionic groups are mainly installed to increase the solubility of the sensitizer (e.g. 9,10-anthraquionone sulfonate salts) in polar media without changing its reactivity in a significant manner are excluded.

2.2 Phenolate Catalyzed Oxyarylation of Olefins with Aryl Halides

The low pKa value of phenol, caused by the charge-stabilizing effect of the benzene ring, allows facile deprotonation in presence of base to afford the phenolate, which is able to undergo photochemical reactions under visible-light irradiation. Xia and co-workers examined several 4-phenylphenol derivatives as potential photocatalysts for the visible-light oxyarylation of olefins upon photoreduction of aryl halides (Scheme 5).[71] 4-Phenylphenol PhPH bearing bulky tert-butyl groups adjacent to the phenolic alcohol (see Scheme 6) showed the highest catalytic efficiency and the corresponding oxyarylated products 5 formed in presence of aryl halides 3, olefins 4 and TEMPOH could be isolated in moderate to good yields. Remarkably, the estimated

excited state oxidation potential of ***PhPH**$^-$ (E^*_{ox} = −3.16 V *vs.* SCE) also allowed to convert more inert and electron rich aryl bromides and chlorides in presence of 4-methoxystyrene. Following the developed procedure, the authors present a broad scope of tolerated (hetero)aryl bromides and iodides including polyaromatic hydrocarbons, pyridines, indoles, quinolines, thiophen, thianaphthene and benzofuran.

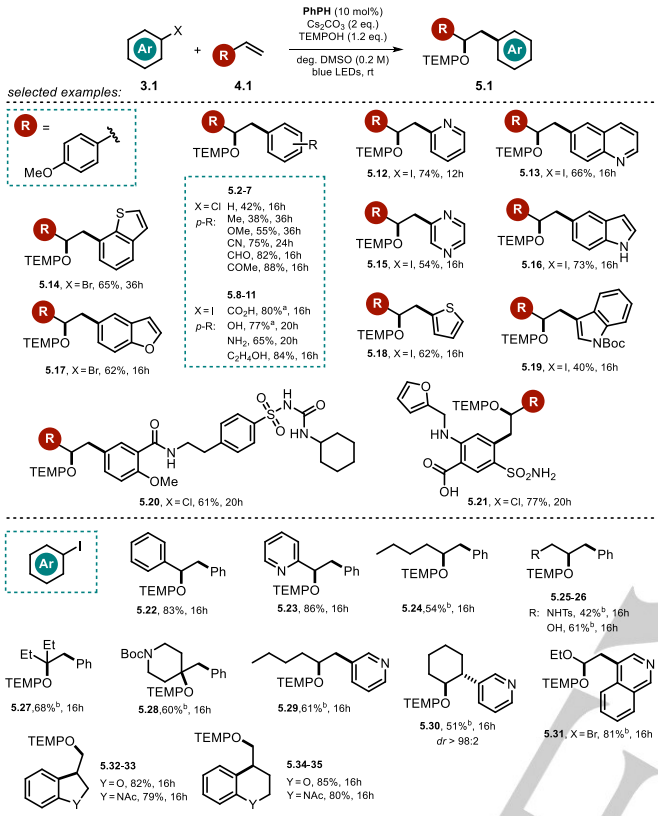

Scheme 5. Scope of the oxyarylation reaction of olefins with aryl halides and TEMPOH. [a]With 3 equiv. of Cs_2CO_3; [b]With 3 equiv. of olefin.

The reaction scope of tolerated olefins comprises various styrenes, aliphatic olefins, allylic sulfonamide and alcohol derivatives, enol ethers as well as 1,1- and 1,2- disubstituted olefins. In addition, the method allowed for intramolecular cyclization reactions using aryl iodides and for the late-stage modification of pharmaceuticals. Noteworthy, the use of TEMPOH as H-atom donor and radical trap seems to be crucial due to the weak nature of the O−H bond and the high stability of the aminoxyl radical formed. The proposed reaction mechanism involves the deprotonation of the phenol **PhPH** by base and a PET from the photoexcited ***PhPH**$^-$ to the aryl halide **3.1**. Upon cleavage of the halide anion, the resulting aryl radical is trapped by the olefin **4.1** causing a carbon centered radical **3.1b**$^\bullet$. Hydrogen atom transfer between the oxidized species of the catalyst and TEMPOH recovers **PhPH** and causes the stable radical TEMPO$^\bullet$. The oxyarylation product **5.1** is formed upon radical-radical coupling (Scheme 6). The formation of a ground-state electron donor acceptor complex (EDA) between phenolate anion and aryl halide was excluded by UV-vis measurements. Fluorescence quenching experiments and isolated TEMPO-trapping adducts of the aryl radical intermediate support the mechanistic hypothesis. Moreover, a radical clock experiment suggests the formation of a benzylic radical, whereas intramolecular trapping experiments disprove the involvement of a benzylic carbocation formed upon oxidation of the radical **3.1b**$^\bullet$.

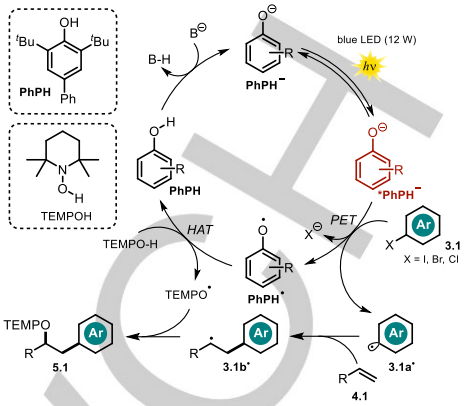

Scheme 6. Proposed mechanism for the phenolate catalyzed oxyarylation of olefins *via* the generation of aryl radicals.

2.3 Naphtholate-Catalyzed Dehalogenation and Detosylation

The first studies of the photochemical behavior of 2-naphtholate anion **NA**$^-$ date back to 1989, when the countercation, temperature and solvent were systematically evaluated regarding effects on the luminescence lifetime and the absorption and emission maxima.[10] In the same year, Soumillion and co-workers demonstrated the application of the naphtholate anion in the photocatalyzed defunctionalization of 2-chloronaphthalene and 4-chlorobiphenyl (**6.2-3**) in degassed, alkaline MeOH (Scheme 7, left).[72]

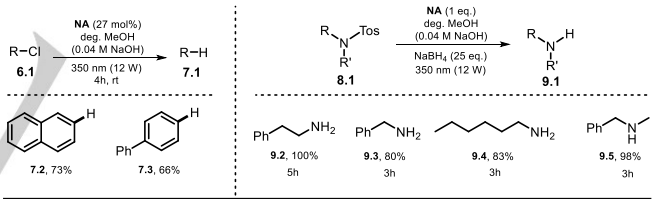

Scheme 7. Scope of the **NA**$^-$-catalyzed dechlorination (left) and desulfonylation reactions (right).

This concept was further extended in a heterogenous approach where 2-hydroxynaphthoic acid was covalently anchored to a silica surface *via* amidation reaction. The efficiency of the dechlorination however was significantly decreased.[73] The substrate scope was later broadened to mono- and dichloronitro-benzenes.[74] In addition, **NA**$^-$ was shown to catalyze the detosylation of sulfonamides in presence of excess $NaBH_4$ as terminal reductant (Scheme 7, right).[75] Following this procedure, 2-phenylethylamine (**9.2**) and *N*-methylbenzylamine (**9.5**) were obtained in quantitative yield starting from the respective sulfonamides. Although a stoichiometric amount of 2-naphthol (**NA**) was utilized, the catalyst could be efficiently regenerated. The proposed reaction mechanism suggests the deprotonation of **NA** to form the naphtholate **NA**$^-$. Upon excitation with blacklight the photoexcited state of ***NA**$^-$ is oxidatively quenched by either aryl chloride or sulfonamide, which causes the formation of **NA**$^\bullet$ and an arene radical anion. After cleavage of the respective anionic leaving group (Cl^- or 4-Me(C_6H_4)SO_2^-), an aryl- or nitrogen centered radical is formed respectively. Abstraction of a hydrogen atom from the solvent affords the defunctionalized

arene. The *N*-centered radical converts to the amine *via* H-atom abstraction from either the solvent or $NaBH_4$. To close the catalytic cycle, **NA•** is transformed to **NA** *via* hydrogen atom abstraction from the solvent or $NaBH_4$, followed by subsequent deprotonation (Scheme 8).

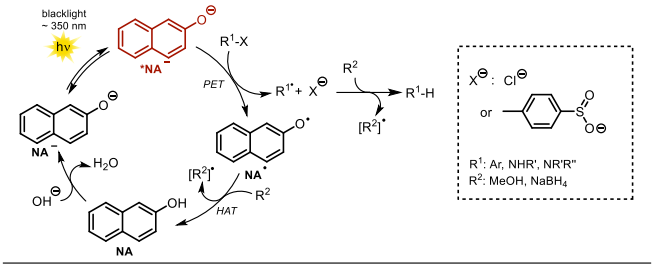

Scheme 8. Proposed photocatalytic cycle for the naphtholate anion.

Recently, a zwitterionic visible-light-absorbing benzimidazolium naphtholate **BINA** was successfully employed in photocatalytic deiodination and desulfonylation reactions in presence of a combined electron and hydrogen atom donor **10** (see Scheme 10).[76] The cationic benzimidazolium moiety can be considered as separated from the naphtholate, due to the tilted structure that prevents π-conjugation. The photocatalytic activity was studied using different solvents with attributed Lewis-basic or Lewis-acidic character estimated by donor and acceptor numbers. The authors concluded that Lewis-basic solvents cause tight interactions with the Lewis-acidic benzimidazolium moiety, whereas the electronic properties of the Lewis-basic naphtholate anion are less governed, resulting in an increased electron donating ability. The best results (Scheme 9) were found using DMF as solvent. Utilizing 10 mol% of catalyst **BINA** and 1.2 eq. of **10** enabled the formation of cyclized **12** in 82% yield. A lower catalyst loading of only 1 mol% resulted in full conversion of the iodoarene **11**, however the product yield was lowered (69%). In addition to the cyclization of iodoarene, the photocatalytic reactivity was demonstrated based on the reductive desulfonylation of tertiary sulfonamides **13** and *β*-ketosulfones **15**. The respective secondary amines and desulfonylated ketones were obtained in good yields. The proposed photocatalytic cycle is depicted in Scheme 10.

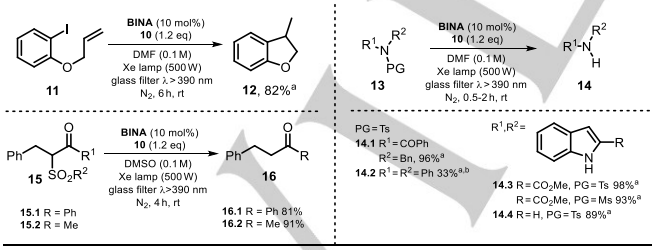

Scheme 9. Cyclization of iodoarene and scope of desulfonylation. [a]NMR yields; [b]DMSO, 6 h.

Upon photoexcitation (λ > 390 nm), the zwitterionic excited state catalyst ***BINA** (E^*_{ox} = −2.08 *vs.* SCE) reduces **11** *via* PET. Subsequent cleavage of iodide followed by fast 5-*exo*-*trig* cyclization affords the primary radical **11b•**. The oxidized photocatalyst **BINA•** is regenerated in presence of a sacrificial reductant **10** ($E_{1/2}$= +0.34 V *vs.* SCE) *via* single electron transfer to give the radical cation **10•+**, which acts as hydrogen atom donor to form **12** and in turn is converted to the cation **10+**. In presence of other terminal reductants *e.g.* Hantzsch ester ($E_{1/2}$= +0.93 V *vs.* SCE) no product was formed as the higher ground state oxidation potential renders an electron transfer towards **BINA•** endergonic.

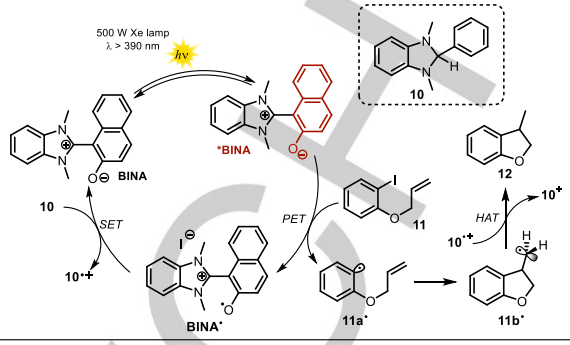

Scheme 10. Proposed catalytic cycle for the radical cyclization of iodoarene in presence of photoexcited benzimidazolium naphtholate.

In previously published work, photoexcited 1,3-dimethyl-2-hydroxynaphthylbenzimidazoline (**BIA-H.1**) was found to convert *N*-sulfonamides and *N*-sulfonylamines into the respective desulfonylated products.[77] Based on these results, Hasegawa *et al.* further developed the catalytic system depicted in Scheme 10 by utilizing the *in situ* reduction of benzimidazolium aryloxides (**BIA**) in presence of readily available boron hydride donors to generate the anionic species **BIA-H⁻**.[78]

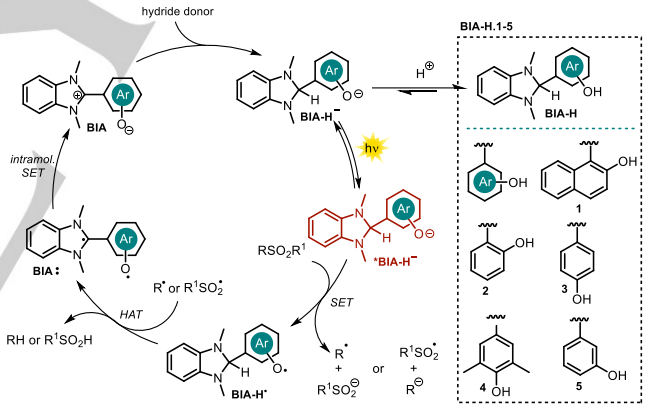

Scheme 11. Proposed photocatalytic cycle for the desulfonylation reported by Hasegawa *et al.*

In addition to the reported electron donor and hydrogen atom donor abilities of the benzimidazoline scaffold (*cf.*, Scheme 10, **10**), the resulting benzimidazoline aryloxides **BIA-H⁻** are equipped with a photoredox active unit, the aryloxide moiety. Reductant, H-atom donor and photocatalyst are thus combined in one molecule. Various benzimidazoline aryloxides **BIA-H.1-5** (Scheme 11) were synthesized and characterized regarding their spectroscopic and electronic properties.[78] The calculated excited state oxidation potential for **BIA-H.1⁻** (E^*_{ox}= −2.71 V *vs.* SCE) was found to be significantly enhanced compared to the zwitterionic species **BINA**, allowing the conversion of less activated substrates. The elaborated protocol was used for the reductive desulfonylation of *N*-sulfonylindoles, -amides, -amines, and α-sulfonyl ketones, affording the unprotected secondary amines as well as the α-defunctionalized ketones in good to excellent yield (Scheme 12).

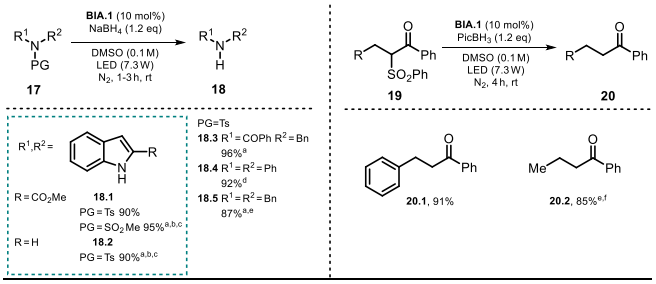

Scheme 12. Scope of the desulfonylation. [a]NMR yield; [b]DMF; [c]Xe lamp (500 W), glass filter > 390 nm; [d]24 h; [e]2×LED (10.8 W), 48 h; [f]Cs_2CO_3 (1 eq.).

For the desulfonylation of α-carbonyls, a less reactive hydride donor $PicBH_3$ was used to avoid the direct reduction of the carbonyl group. Remarkably, utilizing the developed photocatalytic protocol allowed to convert diphenylsulfonamide (**17.4**) and dibenzylsulfonamide (**17.5**) almost quantitatively in 24 and 48 hours, respectively. Note that both substrates exhibit a challenging reduction potential ($E_{1/2}$ < −2 V *vs.* SCE). All synthesized catalysts **BIA.1-5** were successfully tested in the desulfonylation reaction of *N*-tosylindole **17.1** but **BIA.1** (or **BINA**, *cf.* Scheme 10) showed superior catalytic activity. Changing the light-source from a xenon lamp (500 W, λ > 390 nm) to a white LED (7.3 W) afforded comparable product yields, but the reaction time increased. No product was formed in the absence of photocatalyst and only traces were found in absence of hydride donor or light. Regarding the mechanism, the authors propose the *in situ* formation of **BIA-H**$^-$ *via* nucleophilic attack of a hydride on the benzimidazolium moiety of **BIA**. Excitation with either Xe lamp or white LED renders the catalyst a strong photo-reductant and allows PET onto the substrate. The open-shell fragment formed upon N-S or C-S bond-rupture abstracts a hydrogen atom from the photocatalyst **BIA-H**$^\bullet$ which is turned into a biradical **BIA:** and, upon intramolecular single electron transfer, the benzimidazolium **BIA** is regenerated. Eventually, a hydride transfer activates the catalyst for another catalytic cycle (Scheme 11). The acidic hydroxy group on the aryl oxide is easily deprotonated and enables to directly employ the benzimidazoline **BIA-H** instead of the betaine **BIA** as catalyst. In that case, the addition of base (sodium carbonate or butoxide) increased the reaction efficiency significantly, indicating a facile deprotonation of **BIA-H**.

2.4 Anthrolate-catalyzed Generation of Hydrated Electrons

Goez and co-workers thoroughly investigated the potential use of anionic 9-anthrolate (**ANT**$^-$) as a sustainable source for hydrated electrons which are ejected upon laser irradiation.[20] Hydrated electrons are among the strongest reductants[79–81] and are capable to directly reduce dinitrogen[82] or carbon dioxide[83]. Approaches to liberate solvated electrons photochemically often rely on high-energetic and harmful UV-C light. Notably, pulsed 355 nm UV-A laser irradiation of **ANT**$^-$ in alkaline aqueous media afforded hydrated electrons *via* a biphotonic photoionization pathway. The first photon generates the excited anionic species (S_1 state) and the absorption of another photon within the excited state lifetime of ***ANT**$^-$ stimulates photo-ejection of a hydrated electron. The catalytic cycle is closed in presence of the ascorbate dianion, which acts as sacrificial reductant recovering the catalyst from its oxidized species **ANT**$^\bullet$ (Scheme 13). The sequence of photoionization and regeneration of the catalyst could be repeated several times until the system was exhausted. At the same time, the initial concentration of the catalyst remained constant, indicating the robustness of anthrolate against an attack of the exceptionally reducing solvated electron. Despite its minute molar absorption coefficient at the wavelength used for exciting the system, the ascorbate dianion **Asc**$^{2-}$ was found to slightly contribute in generating hydrated electrons.

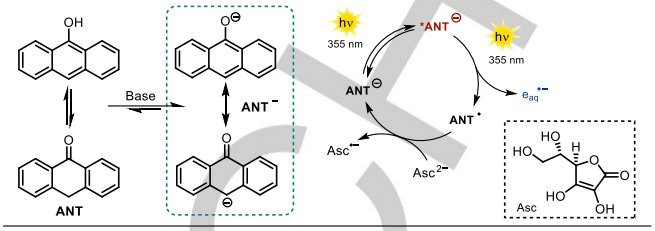

Scheme 13. The photocatalytic generation of hydrated electrons reported by Goez and co-workers.

A follow-up work of the Goez group[21] focused on the direct photoionization of the ascorbate dianion in absence of catalyst by applying a 355 nm laser pulse. A possible application of solvated electrons generated in this way was demonstrated based on the efficient dechlorination of chloroacetate as a generic pollutant in waste water detoxification.

2.5. Activation of Aryl chlorides with 9-Anthrolate

Recently, the photochemical properties and synthetic applications of a series of 9-anthrone derivatives were studied by König and co-workers and the corresponding anions were found to reach remarkable excited-state oxidation potentials.[22]

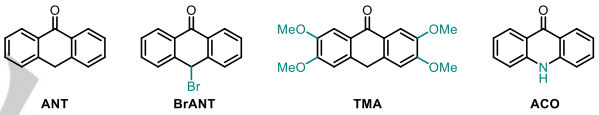

Figure 3. Selected 9-anthrone-based photocatalysts reported by König and co-workers.

In solution, anthrone **ANT** is in equilibrium with its enolic form and is easily deprotonated to give the visible-light-absorbing anthrolate **ANT**$^-$. The most efficient catalysts examined in that work are depicted in Figure 3.

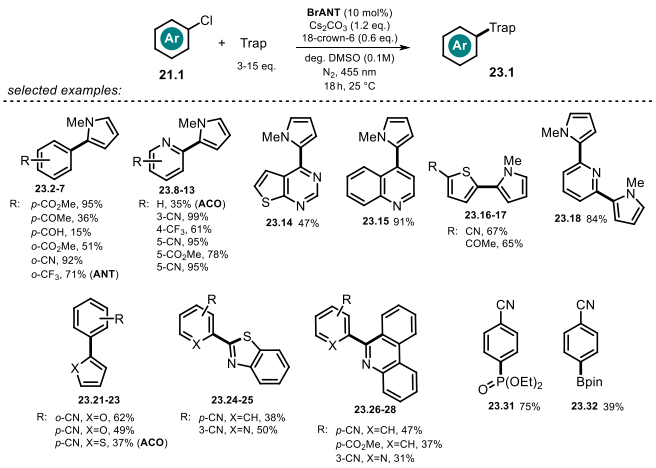

Scheme 14. Scope of the C−H arylation of (hetero)arenes using pyrroles, isocyanides, phosphite and B_2pin_2 as trapping reagents. For some substrates, other catalyst derivatives were used as stated in parenthesis behind the entry.

These photocatalysts were proved successful in catalyzing the C−H arylation reaction of several (hetero)aryl chlorides with electron-rich (hetero)arenes, isocyanides, phosphite and B_2pin_2 (Scheme 14). In presence of base, anthrone **ANT** is deprotonated, which causes a red-shift in the absorption spectrum with a new distinct absorption band arising in the visible range. Upon excitation with blue LED light, the strongly reducing excited anion ***ANT**$^-$ is formed (*cf.*, Table 1, Entry 5 for **ANT**$^-$). Exceeding the reduction potential of the aryl chloride, oxidative quenching of the excited catalyst would form an arene radical anion **21.1**$^{\bullet-}$ and the open-shell **ANT**$^\bullet$. A subsequent mesolytic bond cleavage gives rise to a reactive aryl radical **21.1a**$^\bullet$, which is trapped by an electron rich arene **22**. In alkaline media, the emerging bicyclic radical intermediate gets deprotonated to afford the radical anion **21.1b**$^{\bullet-}$. The catalytic cycle is closed *via* electron transfer from **21.1c**$^{\bullet-}$ to **ANT**$^\bullet$ (Scheme 15). Time-resolved luminescence quenching experiments of the excited photocatalyst **ANT**$^-$ with various tolerated aryl chlorides shortened the lifetime, whereas unsuccessful aryl chlorides caused no quenching.

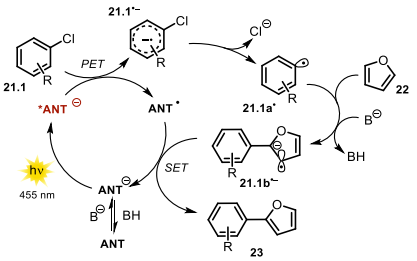

Scheme 15. Proposed mechanism of the photocatalyzed C−H arylation in presence of 9-anthrone.

TEMPO-trapping experiments confirmed the formation of aryl radical 21.1a• and bicyclic radical 21.1b•. Remarkably, in contrast to other photocatalyzed procedures for aryl halide activation[37–40,52,84] no sacrificial electron donor (e.g. DIPEA) was necessary and the scope of aryl chlorides as well as tolerated radical trapping reagents could be broadened. In the model reaction, the catalyst loading could be lowered to 5 mol% (92% yield) which indicates a turn-over number greater than 18. In accordance with recently reported photocatalyzed C−H arylation procedures[37–40,84] it was found that excess of the trapping reagent is crucial for the reaction outcome, as a stoichiometric amount with reference to the aryl halide resulted in significantly decreased product yield. Anthrolates are converted in presence of oxygen yielding the corresponding anthraquinones, thus reactions were carried out under inert atmosphere. Noteworthy, acridone (ACO) afforded the desired arylation product 23.2 in good yield (83%) in non-degassed solvent and in presence of air, indicating an increased stability in presence of oxygen.

2.6. Anthrolate Catalyzed C−H Carboxylation of (Hetero)arenes and Styrenes with CO_2

Very recently, the visible-light-absorbing, strong photo-reductant tetramethoxyanthrolate **TMA**$^-$ (E^*_{ox} = −2.92 V *vs.* SCE) was utilized to achieve the photocatalytic direct reduction of (hetero)arenes and styrenes to their respective radical anions.[85] The associated nucleophilic character of such electron rich species was exploited in C−H carboxylation reactions with gaseous CO_2 affording the aromatic carboxylic- and cinnamic acids in moderate to excellent yields. Among others, non-prefunctionalized naphthalenes, thiophenes, furans, indoles, pyrazoles and styrenes are converted to the corresponding carboxylic acids under exceptionally mild reaction conditions (Scheme 16). An examined gram scale carboxylation of 2-cyanothiophene **26.9** illustrates the ease to scale-up this reaction. Moreover, a late-stage C−H carboxylation of a Boc-protected thiophene analogue of propranolol **26.31** is demonstrated following this procedure. Besides CO_2, ketones were found to convert to the corresponding tertiary alcohols (**26.32-33**) following the same approach. Noteworthy, similar transformations usually require stoichiometric amounts of reactive organolithium reagents and are conducted under low temperature (−78 °C). Thus, a former protection of labile functional groups is often required, leading to a multi-step synthesis.[86–88]

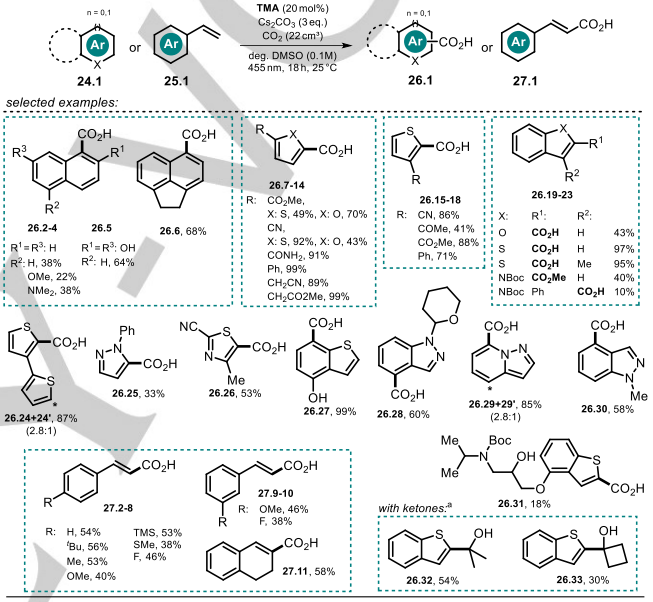

Scheme 16. Photocatalyzed C−H carboxylation of (hetero)arenes and styrenes and hydroxyalkylation of thianaphthene. [a]Reaction with ketone (10 eq.) and under nitrogen atmosphere in absence of CO_2.

The regioselectivity of the carboxylation reaction can be predicted by theoretical means. In contrast to the carboxylation mediated by organometallic reagents, the reported photocatalyzed, redox-neutral insertion of CO_2 into non-activated sp^2-hybridized C−H bonds benefits from increased regioselectivity, giving rise to only one regioisomer **26.18** and **26.25**, respectively. In presence of base, **TMA** is in equilibrium with the anionic form, which in contrast to the neutral species shows distinct absorption in the visible range. Excitation with a blue LED generates the excited state of the anionic catalyst ***TMA**$^-$ which acts as a remarkably strong photo-reductant. Upon SET, benzothiophene **24.20** is reduced to the resonance stabilized radical anion **24.20**$^{\bullet-}$. Subsequent nucleophilic attack affords the carboxylate **24.20a**$^{\bullet-}$. The closure of the catalytic cycle is proposed to occur *via* an electron-rich radical dianion intermediate **24.20b**$^{\bullet 2-}$, formed upon deprotonation of **24.20a**$^{\bullet-}$, which regenerates the active anionic catalyst by single electron transfer causing the carboxylate **24.20c**$^-$. Eventually, acidic work-up affords the carboxylic acid **24.20** (Scheme 17). An alternate pathway *via* direct H-atom abstraction from **24.20a**$^{\bullet-}$ caused by the open-shell species **TMA**$^\bullet$ is also conceivable. In both cases, the gain in energy upon re-aromatization of the compound is considered as the driving force to close the catalytic cycle.

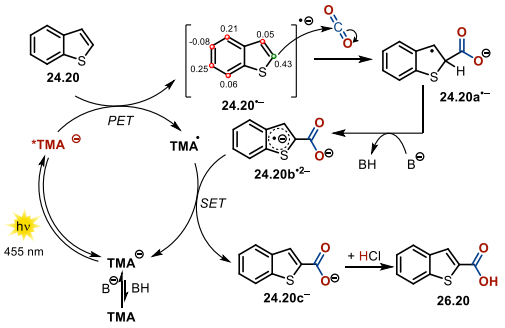

Scheme 17. Proposed reaction mechanism for the redox-neutral, photocatalyzed carboxylation of (hetero)arenes and styrenes utilizing **TMA** as strong photo-reductant. Calculated Mulliken spin populations for **24.20**•− allow to predict the regioselectivity of the carboxylation.

The mechanistic hypothesis was supported by time-resolved luminescence quenching experiments of the catalyst ***TMA**⁻ in presence of (hetero)arenes and styrenes. Tolerated substrates shortened the excited-state lifetime of the photocatalyst and linear Stern-Volmer plots could be developed. Although the direct reduction of CO_2 ($E_{1/2}$ = −2.21 V *vs.* SCE)[89] by the excited catalyst is thermodynamically feasible, a DMSO solution saturated with carbon dioxide was found to scarcely affect the excited-state lifetime. Examined substrates that showed quenching of the photoexcited state of the catalyst however failed to give the respective carboxylic acids are considered to exhibit insufficient nucleophilicity when present as radical anions and thus do not react with carbon dioxide. In addition, deuterium-labelling experiments of **24.21** in presence of D_2O and ^{t}BuOD respectively, caused the incorporation of deuterium into the reactive C-2 position, which supports the assumption of a basic radical anion intermediate.

2.7. Catalytic Reactions of Anionic Metal Complexes

Transition-metal complexes like the Ru(II) polypyridine or the cyclometalated Ir(III) found widespread applications in photocatalysis, as they are photostable, show tuneable redox potentials and their excited state lifetimes are usually durable. In contrast to neutral complexes like *fac*-Ir(ppy)$_3$ or cationic metal-based sensitizers [*e.g.* Ru(bpy)$_3^{2+}$, Ir(ppy)$_2$(dtbbpy)$^+$], anionic transition-metal complexes are barely explored, which could be attributed to photodecomposition with monodentate anionic ligands[90] and the shortage of more stable dianionic ancillary ligands available. Godbert and co-workers were able to synthesize and characterize the anionic iridium complex **28.1** with a dianionic orotate ligand (Scheme 18, top).[91] Later on, the complex was modified by exchanging the 2-phenylpyridine ligands with coumarin-derived ligands (**28.2**) to increase the visible-light absorption. The authors successfully demonstrated the use of **28.2** in visible-light-driven H_2 generation which resembled the first example of a photoinduced electron transfer using an anionic Ir(III) sensitizer.[92]

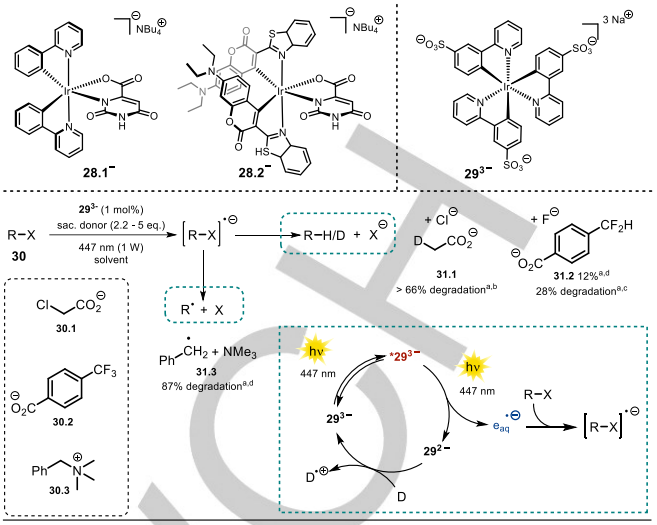

Scheme 18. Negatively charged iridium complexes (top); Irsppy (**29**$^{3-}$) catalyzed degradation of pollutants (center); [a]Conversion was determined by crude NMR; [b]Reaction conditions: Chloroacetate 61.1 (12.5 mM), NaHAsc (2.2 eq.) in D_2O (3 mL), 4 h; [c]Reaction conditions: Trifluormethyl arene 61.2 (15 mM), TEOA (5 eq.) in H_2O (16 mL), 4 h; [d]Reaction conditions: Benzyltrimethylammonium salt 61.3 (10 mM), TEOA (5 eq.) in D_2O (3 mL), 3 h. Proposed catalytic cycle for the generation of hydrated electrons (bottom right).

Based on the well-established *fac*-Ir(ppy)$_3$ Wenger and co-workers utilized a trisulfonated analogue **29**$^{3-}$ (Scheme 18, top), which renders the sensitizer water-soluble and negatively charged, to generate hydrated electrons.[93] A potential use of hydrated electrons in waste water treatment was demonstrated by the degradation of chloroacetate (Scheme 18, **31.1**) and benzyltrimethylammonium salt (**31.3**). In addition, the defluorination of trifluoromethylbenzoate is possible in presence of such a strong reductant (**31.2**). The catalytic cycle is depicted in Scheme 18 (bottom right). The photocatalyst is excited with a 447 nm collimated diode laser. Remarkably, the absorption of a second photon stimulates the ejection of the electron within the lifetime (≈1.6 µs) of the excited sensitizer. The photocatalyst is then regenerated by either sodium ascorbate or triethanolamine acting as sacrificial electron donors. Compared to the neutral *fac*-Ir(ppy)$_3$, the excited state oxidation potential of the anionic sensitizer **29**$^{3-}$ (E^*_{ox} = −1.89 V *vs.* SCE) was found to be slightly increased.

The trianionic, rare-earth-metal catalyst hexachlorocerate(III) **[Ce^{III}Cl$_6$]$^{3-}$** was found to be effective in the reductive dehalogenation of aryl halides **32.1** using UVA light (Scheme 19).[94] This complex is stable to air and moisture and can be generated *in situ* by mixing $CeCl_3$ and NEt_4Cl in acetonitrile. Blacklight irradiation causes a metal centered excited state with very negative potential (E^*_{ox} ≈ −3 V *vs.* SCE)[95,96] enabling a PET to the aryl halide **32.1** to afford a Ce^{IV} species. Interestingly, the reaction could also be performed with a catalytic amount of $CeCl_3$, owing to the complementary oxidative photochemistry of **[Ce^{IV}Cl$_6$]$^{2-}$** (Scheme 19, right).[97] The addition of toluene (**34**) as the terminal reductant allowed to close the catalytic cycle in which it is converted to benzyl chloride **34b** upon hydrogen atom abstraction and reaction with $Cl_2^{\bullet-}$.

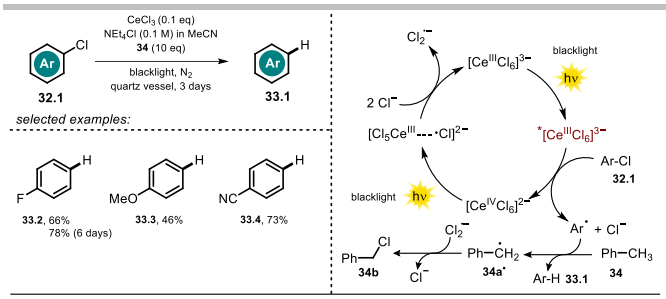

Scheme 19. Scope of the $CeCl_3$ catalyzed defunctionalization of aryl halides by the *in situ* formation of **[Ce^{III}Cl$_6$]$^{3-}$** and a conceivable mechanism for the reaction.

In a follow-up work, the developed catalytic protocol was utilized for the photoinduced Miyaura borylation of aryl bromides and chlorides. Schelter and co-workers used diboron esters which functioned as both borylation reagent and terminal reductant to close the catalytic cycle.[98] Various arylboronic ester could be obtained in moderate to good yields starting from substituted (hetero)aryl chloride derivatives (Scheme 20). Notably, Stern-Volmer quenching experiments revealed that both electron deficient and electron rich substrates do quench the luminescence of the cerium catalyst. The authors also demonstrated that a sequential borylation and subsequent Pd-catalyzed cross-coupling reaction of the formed arylboronic ester is possible. This procedure is beneficial as it avoids prior isolation of the boronate ester. Based on spectroscopic investigations and experimental findings, a reaction mechanism was proposed (*cf.* Scheme 19). The *in situ* formed **[Ce^{III}Cl$_6$]$^{3-}$** gets photoexcited by blacklight. Upon PET towards **35.1** and loss of Cl^-, an aryl radical is formed which reacts with the diboron ester **36.1** to yield the aryl boronic ester **37.1** and a boryl radical $B(OR_2)^{\bullet}$. The oxidized catalyst is regenerated in presence of excess Cl^- *via* photoinduced ligand-to-metal charge transfer giving rise to the radical anion $Cl_2^{\bullet-}$. A reaction quantum yield $\Phi > 1$ was found by actinometry indicating a radical chain mechanism however, no product formation within the dark periods of an intermittent-light experiment was observed. The authors consider the boryl radical, which is stabilized in presence of Cl^-, to presumably propagate a chain mechanism *via* reaction with another substrate molecule.

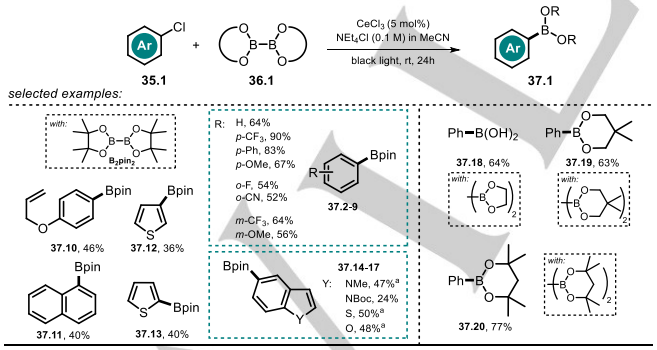

Scheme 20. Scope of the **[Ce^{III}Cl$_6$]$^{3-}$** catalyzed Miyaura borylation. [a]Aryl bromide was used.

2.8. Polyoxometalates as Photocatalysts

Polyoxometalates (POMs) are a class of widely studied molecular metal oxide anions. Their robustness upon irradiation renders them attractive candidates as catalysts. The discussion of POM photocatalysis will be limited herein to recent, selected examples of the decatungstates, routinely employed as sodium (**NaDT**) or tetrabutylammonium salt (**TBADT**, see Scheme 22). Hence, for a comprehensive study of POM chemistry we refer the interested reader to excellent reviews.[99–103] Despite being negatively charged, these metal oxide anions act as strong oxidants from their excited states. This rare feature might be explained analogously to what was discussed for eosin Y and fluorescein (*vide supra*). Tungsten is present in its highest oxidation state (+VI) while the negative charge is centered on the oxygen atoms of the cluster, rendering the metal center highly electron poor and prone to reduction. Upon photoexcitation, a ligand to metal charge transfer (O → M) is proposed, generating a relaxed excited state cluster $[W_{10}O_{32}]^{4-*}$ which is easily reduced (E^*_{red} = +2.44 V *vs.* SCE)[99]. Besides electron transfer reactions, excited decatungstate found widespread interest for its ability to abstract hydrogen atoms from non-activated C(sp^3)−H bonds. Fagnoni, Ryu and co-workers summarized site-selective C−H functionalizations of alkanes, alcohols, ethers, ketones, amides, esters, nitriles and pyridylalkanes by using decatungstate and explained the observed regioselectivities based on polar and steric effects.[104] In 2018, MacMillan and co-workers demonstrated the powerful merger of anionic decatungstate photocatalysis and transition metal-catalyzed cross-coupling.[105] Based on this methodology, a copper/decatungstate dual catalytic approach was recently developed enabling the C(sp^3)−H trifluoromethylation of various biorelevant compounds including natural products and medicinal agents in moderate to good yield (Scheme 21).[106] Note, that the introduction of a CF_3-group into drug molecules often improves pharmacokinetic properties and is therefore of interest. In case of pyrrolidine (**40.2**) selectivity for the CF_3-functionalization is achieved upon protonation of the amine resulting in stronger and less hydridic α-C−H bonds and thus enabling reactivity at the distal position. Regioselective functionalization was found at the benzylic (**40.5**-**40.6**, **40.9**) or sterically most accessible, electron-rich C(sp^3)−H bond (**40.3**, **40.7**). The reaction is initiated by 390 nm light, causing an electrophilic oxometallate excited state. Upon hydrogen atom abstraction of the β-C(sp^3)−H bond of the protonated pyrrolidonium species **38.2**$^+$, the reduced decatungstate catalyst **H$^+$[W$_{10}$O$_{32}$]$^{5-}$** and the aliphatic radical cation **38.2**$^{\bullet+}$ are formed. Subsequent single electron transfer towards Togni reagent II **39** regenerates the active HAT catalyst and enables the formation of a copper(II)−CF_3 species **41.2**. The pyrrolidonium radical **38.2**$^{\bullet+}$ is captured by the copper complex to form an alkyl−copper(III)−CF_3 intermediate **41.3** and eventually the product **40.2** is formed upon reductive elimination and regeneration of the Cu(I) catalyst **41.1** (Scheme 22).

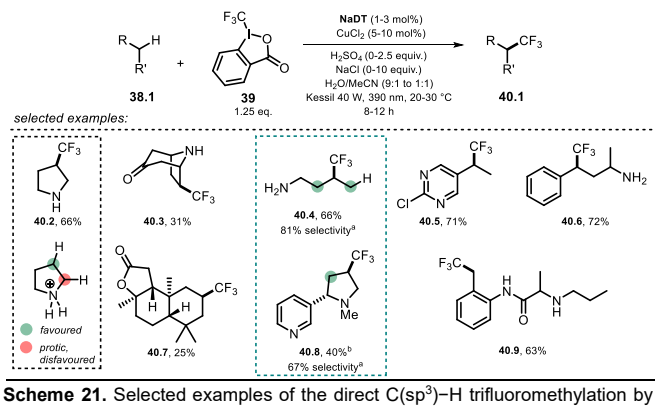

Scheme 21. Selected examples of the direct C(sp^3)−H trifluoromethylation by merging decatungstate catalysis and copper catalysis. [a]The selectivity is reported as the percentage of the major regioisomer over all regioisomers formed; [b]major diastereomer shown.

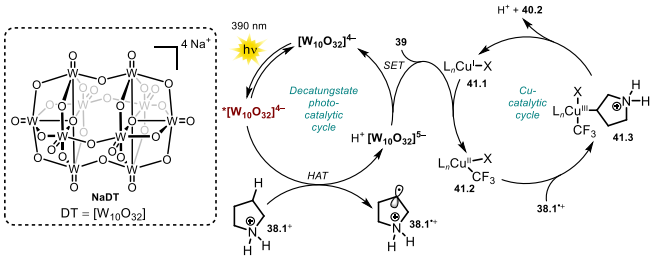

Scheme 22. Proposed dual-catalytic mechanism for the direct C(sp^3)–H trifluoromethylation.

Wu and co-workers disclosed the oxidant-free, site- and *E*-selective dehydrogenative alkenylation of alkanes or aldehydes with alkenes by combining decatungstate HAT photocatalysis and cobaloxime catalysis.[107] This dual-catalytic strategy enables efficient and direct alkenylation of C–H bonds with hydrogen gas being the sole by-product. A broad range of alkanes and aldehydes could be alkenylated. Notably, aryl halides (Cl, Br, I) alkyl bromides, alkenes and alkynes were tolerated which enables subsequent orthogonal functionalization *via* transition-metal catalysis. Moderate to good regioselectivity was observed for alkane substrates **42.13-14** and **42.19**. In addition, the concept could be employed to the late-stage alkenylation of natural products (Scheme 23).

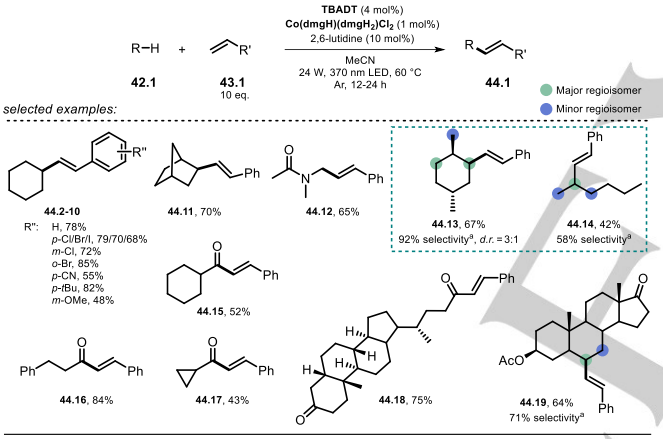

Scheme 23. Selected examples of the dehydrogenative alkenylation of alkanes and aldehydes with styrene derivatives. [a] The selectivity is reported as the percentage of the major regioisomer over all regioisomers formed.

The excitation of the metal oxide cluster $[W_{10}O_{32}]^{4-}$ (**TBADT**) enables the abstraction of a hydrogen atom from alkanes or aldehydes **42.1** and subsequent addition of the resulting carbon-centered radical **42.1a**• to an alkene **43.1** would furnish intermediate **42.1b**•. This species is expected to be reversibly captured by the Co(II)-complex **45.1** to form the alkyl-Co(III) intermediate **45.2**.

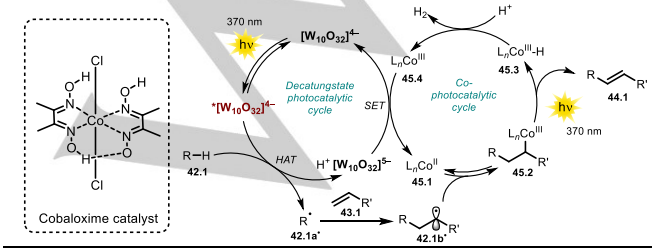

Scheme 24. Proposed dual-catalytic mechanism for the dehydrogenative alkenylation of alkanes and aldehydes with alkenes.

Upon light-mediated formal *β*-H elimination the product **44.1** and Co(III)–H species **45.3** is formed, which reacts with a proton to release H_2 and the Co(III)-complex **45.4**. Eventually the decatungstate and the cobalt catalyst are regenerated *via* SET (Scheme 24).

Wang *et al.* recently published the **TBADT**/Ni dual-catalytic asymmetric acyl-carbamoylation of tethered alkenes using a chiral nickel catalyst to form oxindole motifs bearing a quaternary stereogenic center **49.2-5** (Scheme 25).

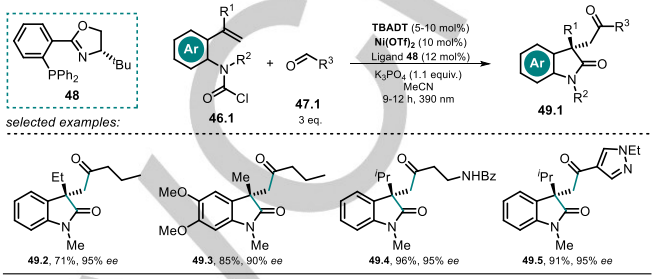

Scheme 25. Selected examples of the asymmetric acyl-carbamoylation.

The reaction starts with H–atom abstraction from the aldehyde by the excited decatungstate catalyst ***[W10O32]4–*** and the resulting acyl radical **47.1a**• is captured by *in situ* formed Ni(0) to yield an acyl Ni(I) intermediate **50.2**. Oxidative addition of the carbamoyl chloride to **46.1** causes a Ni(III) species **50.3**. In the enantioselective step, migratory insertion to the tethered double bond takes place (**50.4**) and subsequent reductive elimination affords the cyclized product **49.1** along with Ni(I) chloride **50.5**. Both catalytic cycles are closed via SET presumably between the reduced decatungstate **$[W_{10}O_{32}]^{6-}$** and Ni(I)Cl **50.5** (Scheme 26).

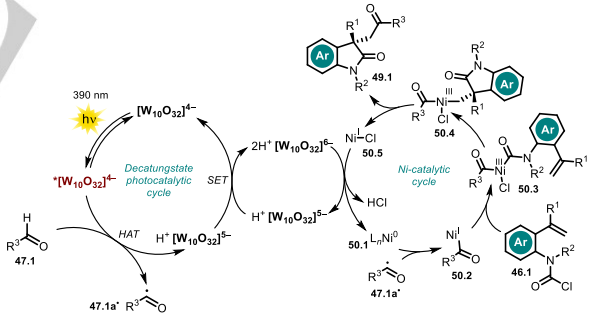

Scheme 26. Proposed dual-catalytic mechanism for the asymmetric acylcarbamoylation using a chiral Ni-complex.

Another example for a light-mediated asymmetric C–H functionalization was recently demonstrated by Pu-Sheng Wang and co-workers.[108] Upon hydrogen atom abstraction by **TBADT**, an alkyl, benzyl or allyl radical adds to an exocyclic enone and the resulting α-carbonyl radical regenerates the photocatalyst *via* hydrogen atom transfer. In the enantioselective step, the formed enol-intermediate is protonated by an aligned chiral spiro phosphoric acid generating a stereocenter in α-carbonyl position.

Based on the synergy of decatungstate HAT catalysis and nickel catalysis, Wang and co-workers demonstrated the acylation of aryl halides and α-bromo acetates with aromatic and aliphatic aldehydes and the resulting aromatic ketones could be obtained in moderate to good yield.[109] In a similar fashion, the group of Zheng disclosed very recently the direct C–H arylation of

aldehydes enabled by merging decatungstate HAT photocatalysis and palladium cross-coupling catalysis.[110] Applying this methodology allowed for the efficient linkage of various (hetero)aryl bromides, iodides and triflates with aromatic and aliphatic aldehydes. Moreover, TBADT was shown to promote H/D exchange reactions of formyl C−H and a wide range of hydridic C(sp^3)−H bonds in a synergistic system comprised of HAT photocatalyst and thiol catalyst. In presence of D_2O, this protocol allowed for the regioselective incorporation of deuterium into pharmaceutical relevant molecules and drug precursors.[111] Furthermore, a few examples are known where polyoxometalates equipped with binding sites on the cluster shell or in presence of co-catalysts participate in reductive CO_2 activation or H_2 generation.[34]

3. Excited Anionic Compounds as Reagents

Besides using a light-harvesting anionic catalyst as demonstrated in Section 2, chemical reactions can also be promoted *via* a direct photoexcitation of anionic reagents which will be discussed in the following part.

3.1 Excited State Phenolate as Photoreductant

Recently, Xia and co-workers made use of the remarkable excited-state potential of the phenolate **52.2** (E^*_{ox} = −2.48 V *vs.* SCE) in a Heck-type arylation reaction promoted by blue LED light.[112]

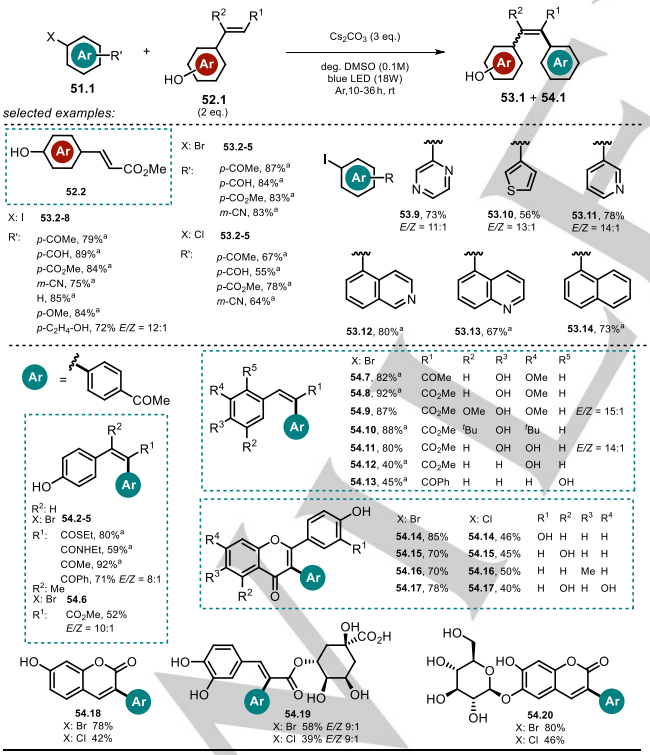

Scheme 27. Substrate scope of the Heck-type arylation reaction reported by Xia and co-workers; [a]*E*/*Z* > 19:1.

The synthetic utility was demonstrated based on the arylation of methyl 4-hydroxycinnamate **52.2** with various (hetero)aryl halides **51.1** (Scheme 27). In addition, other derivatives of cinnamic acid (**52.2-13**, **52.19**), and flavonoids (**52.16-18**, **52.20**) were shown to react smoothly *via* the generated aryl radical to afford the respective arylation products (**53.1** & **54.1**) in moderate to good yields. Remarkably, as the proposed mechanistic cycle is redox-neutral, no sacrificial electron donor is necessary. Besides electron deficient aryl iodides, the scope includes electron rich as well as electron neutral derivatives. In contrast, arylation products formed with less activated aryl bromides and chlorides are only shown with activated, electron deficient arenes. The *E*/*Z* ratios of the formed arylation products are high for most of the isolated compounds. The mild reaction conditions allowed to convert complex, biologically active substrates like chlorogenic acid, esculin and scutellarin. Upon deprotonation of the phenolic OH group, the absorption spectrum of **52.2** in DMSO is shifted towards longer wavelength enabling direct excitation of the phenolate **52.2**$^-$ with blue light. From the photoexcited state ***52.2**$^-$ (Scheme 28) an electron transfer to the aryl halide **51.2** is feasible and subsequent cleavage of bromide forms the reactive aryl radical **51.2a**$^\bullet$, which preferentially couples to electron rich species like the vinylphenolate **52.2**$^-$.

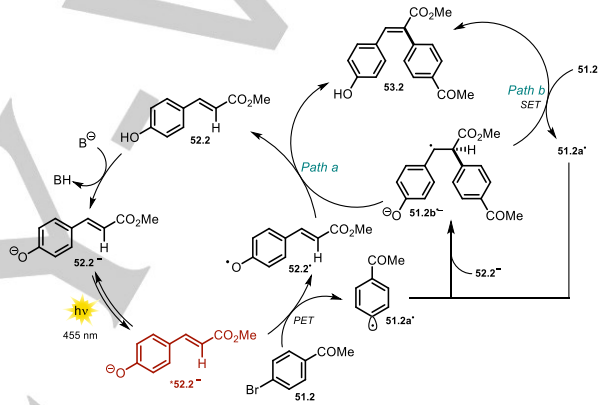

Scheme 28. Proposed reaction mechanisms for the photochemical Heck-type arylation of vinylphenols.

The resulting radical anion **51.2b**$^{\bullet-}$ is assumed to either initiate a radical chain mechanism by reducing another equivalent of **51.2** which affords the desired Heck-type arylation product **53.2** (*Path b*), or is converted to the latter in presence of the phenoxy radical **52.2**$^\bullet$ *via* direct hydrogen atom transfer or electron transfer followed by a proton shift (*Path a*).

Melchiorre and co-workers have recently demonstrated how phenolate can elicit the generation of perfluoroalkyl radicals *via* single electron transfer.[113] The developed method allows for the direct perfluoroalkylation and trifluoromethylation of phenols bearing electron withdrawing substituents **57.2-15** (Scheme 29). In presence of the non-nucleophilic base 1,1,3,3-tetramethylguanidine (TMG) the absorption spectrum of salicylaldehyde (**55.2**) is red-shifted and no change was observed upon addition of the perfluoroalkyl iodide **56.1**, excluding the formation of a ground state EDA complex. The base-induced bathochromic shift allowed for the use of a CFL bulb as light source. Using a 300 W Xe lamp with cut-off filter (λ > 385 nm) still allowed to form the product however in slightly decreased yield. The proposed mechanism of this transformation (Scheme 30) starts with a SET from the photoexcited phenolate ***55.1**$^-$ to **56.1**. Subsequent reductive cleavage of iodine gives rise to a perfluoroalkyl radical **56.1a**$^\bullet$.

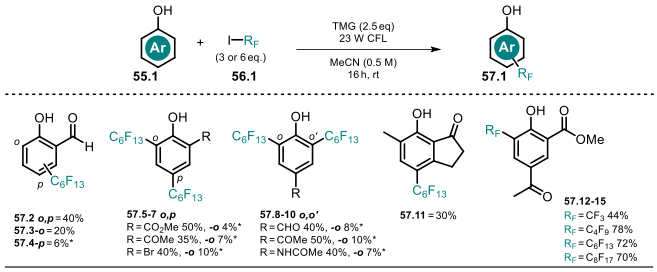

Scheme 29. Scope of the perfluoroalkylation of substituted phenols. Minor positional isomers estimated by crude ^{19}F-NMR are marked with (*); 6 eq. of alkylating agent **56.1** were used for products **57.7-10**.

In the bond-forming step, the radical is trapped by the ground-state phenolate yielding a cyclohexadienyl radical **56.1b**$^{\bullet-}$ which propagates the reaction by reducing another equivalent of **56.1** *via* SET. Subsequent proton shift affords the alkylated phenol **57.1**. Stern-Volmer quenching studies of the phenolate in presence of alkyl iodide support the mechanistic proposal. For *o*-substituted phenols the perfluoroalkylation proceeds with moderate regioselectivity giving rise to *o*-, *p*-monoalkylated and *o*,*p*-dialkylated products, whereas *p*-substituted phenols caused the formation of *o*,*o'*-dialkylated products.

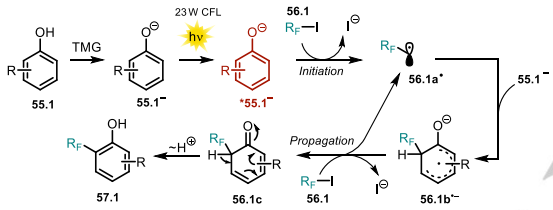

Scheme 30. Light-triggered perfluoroalkylation of phenolates bearing an electron withdrawing substituent by Melchiorre and co-workers. For simplicity, only the *ortho*-alkylation pathway is shown.

Monitoring the product distribution over the reaction time revealed that *o*- and *p*-alkylated products are formed as intermediates and are further converted to bifunctionalized *ortho*, *para*-adducts. Non-substituted or methoxy-substituted phenols as well as nitrophenols failed to convert. Employing phenol **55.12** bearing electron withdrawing groups in *ortho* and *para* position afforded the mono-alkylated product as sole isomer. The demonstrated scope of perfluoroalkyl iodides comprises C_8, C_6, C_4 and C_1 chains (**57.12-15**).

3.2. Visible-light-promoted Arylation of Azaallyl Anions

Chruma and co-workers demonstrated how irradiation of the colored azaallyl anion **58.1**$^-$ with visible light notably increases its excited state oxidation potential.[114] In presence of strong bases (pK_a conjugated acid > 32), the formed 2-azaallyl anion acts as super-electron-donor in the dark[115] and had been successfully employed in the functionalization of non-activated aryl iodides and tertiary alkyl halides.

The accessible substrate scope could be extended by employing visible light causing enhanced reduction potentials and allowed for the conversion of non-activated bromo- and chloro-(hetero)arenes **59.1**, which are present in large excess with reference to **58.1**. The regioselectivity of the arylation reaction is moderate and product mixtures of **60.1** and **61.1** are usually obtained (Scheme 31).

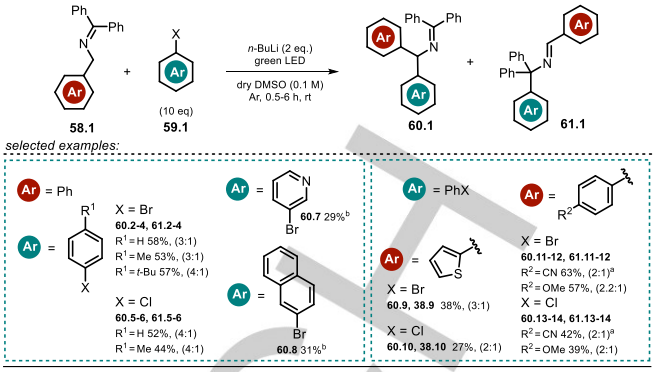

Scheme 31. Scope of the light mediated azaallyl anion coupling with aryl halides. Ratio (**60**:**61**) of the formed regioisomers is given. [a]Blue light; [b]The other regioisomer was not isolated.

The authors propose an electron transfer from the excited state azaallyl anion **58.1**$^{-*}$ to the aryl halide **59.1**. After cleavage of the carbon-halogen bond, a reactive transient aryl radical **59.1a**$^\bullet$ is formed which reacts with the stabilized azaallyl radical **58.1**$^\bullet$ to form the arylation products (Scheme 32).

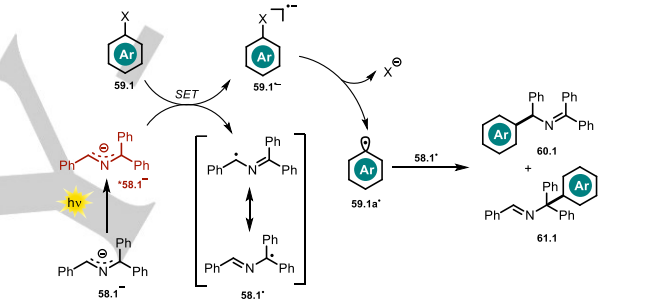

Scheme 32. Arylation of 2-azaallyl anions with non-activated aryl halides.

3.3. Synthesis of Pyrazoles *via* Irradiation of *N*-centered Hydrazone Anions

Zhu and co-workers reported a series of substituted hydrazones **62.1** which are able to undergo cyclization in presence of base, affording pyrazole derivatives **63.1** mediated by sunlight.[116] The UV-vis spectrum of the anionic hydrazone exhibits a significant red-shift compared to the neutral parent, enabling the use of visible light to accomplish the cyclization reaction. Selected examples of formed pyrazoles are depicted in Scheme 33.

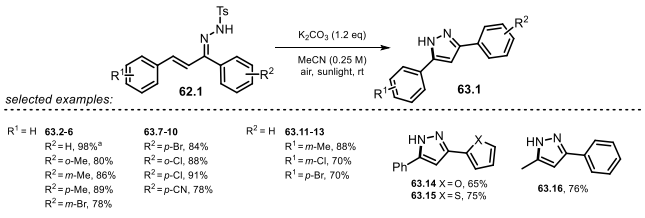

Scheme 33. Selected examples of the formed pyrazoles *via* irradiation of *N*-centered hydrazone anions. [a]Scaled up to 20 mmol reaction.

The authors propose two possible mechanistic pathways (Scheme 34): Deprotonated **62.1**$^-$ gets photoexcited and undergoes either direct anionic cyclization to ***62.1a** (*Path a*) or is oxidized by O_2 to afford the *N*-centered radical **62.1**$^\bullet$ (*Path b*) which, upon intramolecular radical cyclization (**62.1a**$^\bullet$) followed by

cleavage of a tosyl radical, yields the pyrazole **63.1**. Decreased yield is obtained when conducting the reaction under N_2 atmosphere or in presence of the radical trap TEMPO, indicative for the latter mechanistic proposal. Notably, the reactions were also shown to operate in water, however resulted in decreased yields.

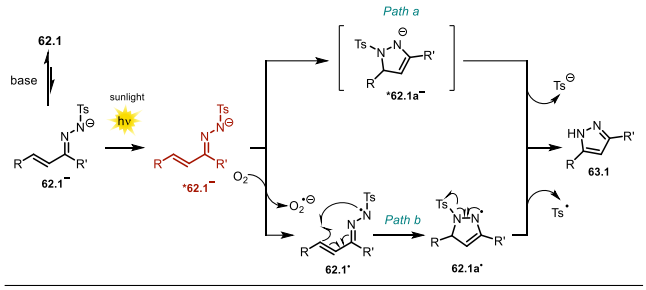

Scheme 34. Proposed photoinduced reaction mechanism towards pyrazole formation.

3.4. Utilizing Phthalimide Anions for H-Atom Abstraction

Already in 1988 the exceptionally high ability of the excited phthalimide anion ***64**⁻ to abstract hydrogen atoms from alcoholic solutions was recognized.[117] This procedure was further developed and could be extended to ethers, alkylbenzenes and amines, affording the reductive addition products with phthalimide (Scheme 35).[118] The use of 4-methylanisole afforded a product mixture (**66.8a-b**) as H-atom abstraction is possible from the methoxy group or in benzylic position. In alkaline solution, phthalimide **64** is in equilibrium with its conjugate base **64**⁻. The photoinduced electron transfer from ***64**⁻ to ground-state phthalimide is a thermodynamically favourable process. Thus, the authors propose the phthalimidyl radical **64**• as the hydrogen atom abstracting intermediate, which evolves from the excited anion ***64**⁻ upon PET towards phthalimide **64**.

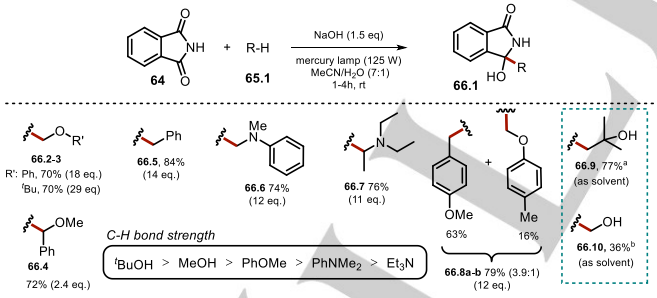

Scheme 35. Light-triggered reductive alkylation of phthalimide. Yields are given on consumed phthalimide. Equivalents used of the hydrogen atom donor are given in brackets. [a]Deviation from reaction conditions: **64** (13.6 mmol), NaOH (16 mL, 1M), ^{t}BuOH (150 mL), mercury lamp (125 W), 5 h; [b]Deviation from reaction conditions: **64** (13.6 mmol), NaOH (10 mL, 1M), MeOH (160 mL), mercury lamp (125 W), 1 h.

Remarkably, the electrophilic radical **64**• is able to activate C−H bonds possessing high bond dissociation energies (*e.g.* ^{t}BuOH, E_{diss} = 100 ± 2 kcal·mol^{-1})[119] and upon hydrogen abstraction, phthalimide **64** and the alkyl radical **65.9**• are formed. Radical-radical coupling between the phthalimide radical anion **64**•⁻ and the carbon-centered radical **65.9**• affords the addition product **66.9** (Scheme 36).

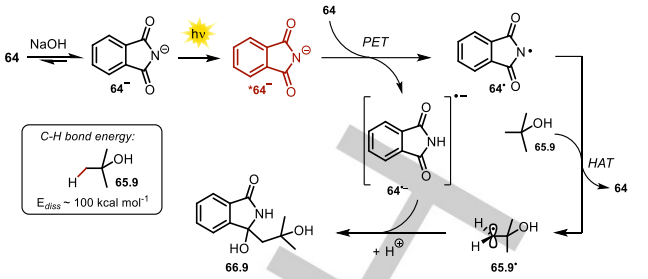

Scheme 36. Light-mediated C−H abstraction and radical addition to phthalimide radical anion **64**•⁻ initiated by the phtalimide radical **64**•.

3.5. Photocycloadditions of Phthalimide and Saccharin Anions

The formation of [2]benzazepine-1,5-dione derivatives **68.1** *via* [2+2] photocycloaddition using phthalimide **64** was previously limited to electron poor non-cyclic alkenes, due to competing excited-state electron transfer reactions.[120,121]

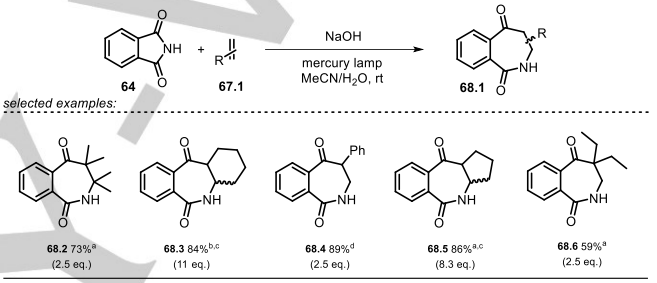

Scheme 37. [2+2] photocycloaddition of excited phthalimide anion with alkenes. [a]**64** (6.8 mmol), NaOH (8 mL, 1M, 1.2 eq.), MeCN/H_2O (160 mL, 7:1), 0.5 h, 125 W mercury lamp; [b]**64** (6.8 mmol), NaOH (pH≈10), MeCN/H_2O (7:1), 0.5 h, 125 W mercury lamp; [c]mixture of *cis*- and *trans*-**68** was obtained; [d]**64** (6.8 mmol), NaOH (10.2 mL, 1M, 1.5 eq), MeCN/H_2O (7:1), 2 h, 400 W mercury lamp.

Suau and co-workers thus mitigated the oxidizing strength by employing the anionic sodium phthalimide **64**⁻ and obtained efficient, regiocontrolled photocycloaddition with a broader range of alkenes being tolerated (Scheme 37). In contrast to the neutral species, **64**⁻ shows significant fluorescence emission, which was markedly quenched upon alkene addition indicating that the singlet excited state ***64**⁻ is the reactive intermediate. The [2+2] cycloaddition of the photoexcited phthalimide anion to double bonds is a stereospecific process yielding the ring expanded *cis*-**68.1** adduct. Epimerization caused by the alkaline media affords a mixture of *cis*- and *trans*-**68.1** (Scheme 38).

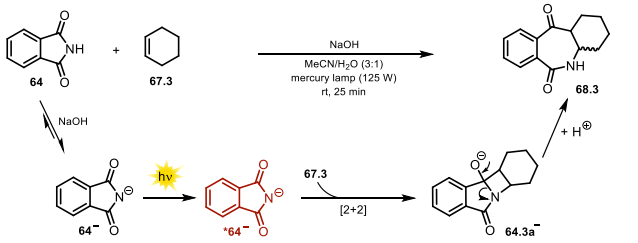

Scheme 38. Proposed mechanism for the [2+2] photocycloaddition of phthalimide anion with cyclohexene.

The photoexcited saccharin anion **69**⁻ was recently found to show similar reactivity towards alkenes, which was utilized in regioselective ring expansion reactions giving benzosultams

71.2-6 (Scheme 39) starting from the cheap and commercially available sweetener saccharin.[122]

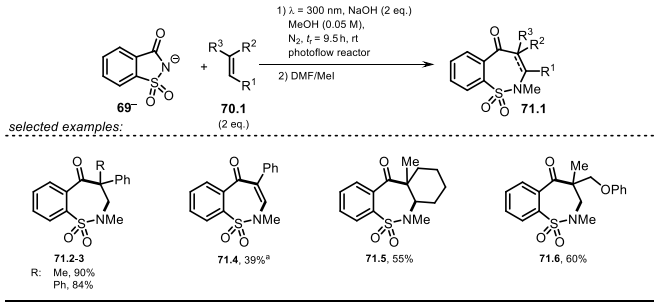

Scheme 39. Selected examples of isolated benzosultams upon ring expansion with alkenes. Reaction conditions: Photoflow reactor 0.75 mm internal diameter. [a]Phenylacetylene was used.

Remarkably, common approaches to form benzo-fused seven-membered sultam derivatives are multistep reactions and rely on the use of toxic organotin hydrides[123] or expensive Pd catalysts[124]. A mechanism was proposed based on experimental and computational studies, suggesting the prevailing population of the S_2 state upon irradiation of the saccharin anion **69**$^-$. The computed data indicate a fast deactivation into the first singlet state. Presumably, the key step towards benzosultam formation is a nucleophilic attack of the nitrogen of the excited state saccharin anion to the alkene. Moreover, no evidence for an azetidine intermediate (*cf.*, **64.3a**$^-$, Scheme 38) resulting from [2+2] cycloaddition of saccharin and alkene was found neither in experiment nor in computational analysis. The C−C bond formation between carbonyl group and alkene is expected to occur in the ground state. Regioselectivity is gained due to the kinetic preference of the nucleophilic nitrogen atom to attack at the terminal, sterically less hindered side (Scheme 40).

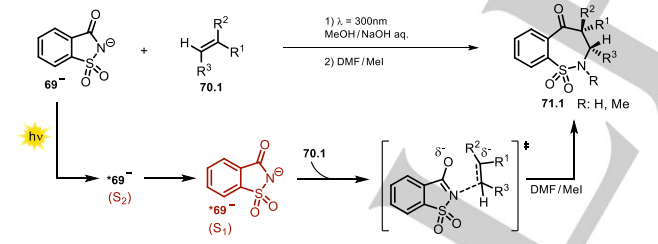

Scheme 40. Proposed reaction mechanism for the light-promoted formation of benzosultams.

3.6. Organic Anions involved in Donor-Acceptor Complexes

Organic anions are also reported to form ground-state electron donor-acceptor (EDA) complexes with electron deficient species usually accompanied by the appearance of a new red-shifted charge-transfer absorption band. During the last years, EDA photochemistry has become increasingly popular. Among others, we highlight herein three examples to demonstrate the concept of organic anions participating in EDA complex formation. For a more detailed study we refer to recent excellent reviews.[125,126] The aromatic perfluoroalkylation of α-cyano arylacetates **72.1** developed by Melchiorre and co-workers[127] is mediated by visible light (CFL 23 W) although neither enolate **72.1**$^-$ nor perfluoroalkyl iodide **56.1** or TMG show absorbance in that range of light. Mixing all the reagents together however results in a colored solution featured by a strong bathochromic shift in the absorption spectrum indicative for the formation of an EDA complex. Irradiation of *p*-substituted substrates allowed to perfluoroalkylate α-cyano arylacetates selectively in *ortho* position.

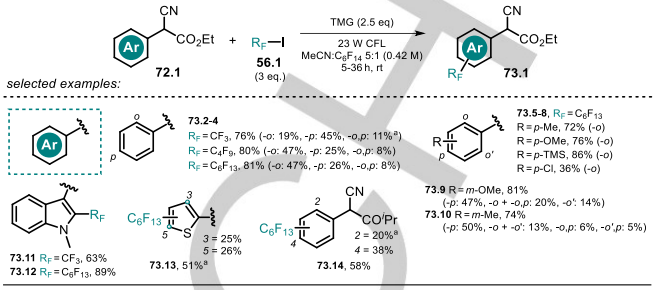

Scheme 41. Selected examples for the perfluoroalkylation of (hetero)arenes. [a]Yield determined by ^{19}F-NMR.

A mixture of regioisomers was obtained when *m/o*-substituted substrates were employed. In accordance with the proposed homolytic aromatic substitution (HAS) pathway lower yields were obtained with electron deficient arenes. Following the developed protocol, the substrate scope could be extended including heteroarenes and α-cyano phenylketone (Scheme 41). Control experiments revealed that the formed product inhibits the reaction as the forming enolate **73.1**$^-$ outperforms the absorbance of the EDA complex. This issue was addressed by utilizing a biphasic system consisting of tetradecafluorohexane and MeCN, which allowed for higher yields and a shorter reaction time.

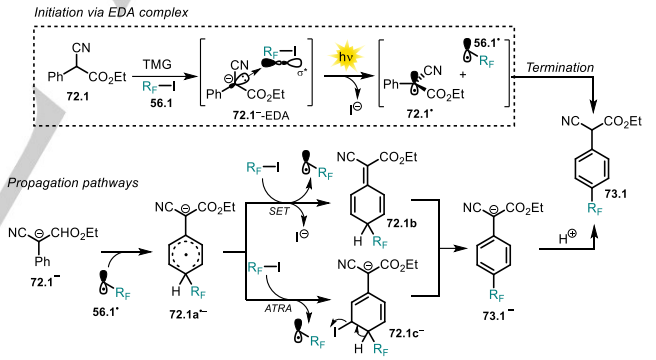

Scheme 42. Proposed reaction mechanism for the perfluoroalkylation of α-cyano arylacetates involving the formation of a visible-light-absorbing EDA complex.

The radical chain reaction is initiated by the base-promoted formation of the EDA complex **72.1**$^-$-EDA, which absorbs visible light and releases a radical pair upon reductive cleavage of iodine consisting of the benzylic radical **72.1**$^•$ and a perfluoroalkyl radical **56.1**$^•$. The electron rich enolate **72.1**$^-$ reacts with the alkyl radical *via* HAS to afford the radical anion intermediate **72.1a**$^{•-}$. Chain propagation is assumed either by SET affording **72.1b** or *via* atom-transfer radical addition (ATRA, **72.1c**$^-$) followed by cleavage of HI. Reaction work-up yields the perfluoroalkylated product **73.1**. Termination of the radical chain is possible upon direct radical-radical coupling of **72.1**$^•$ and **56.1**$^•$ (Scheme 42).

The Miyake group made use of the EDA complex formed between an electron rich thiolate anion **74.1**$^-$ and aryl halides **75.1** to afford a broad scope of aromatic thioethers **76.1**.[128] The

protocol allowed to convert both electron rich and poor thiophenols under visible-light irradiation and in presence of caesium carbonate (Scheme 43). Remarkably, tolerated aryl halides are not limited to activated, electron-deficient arenes, as thioethers were formed with iodobenzene and toluene; however, a prolonged reaction time was required (20-24 h).

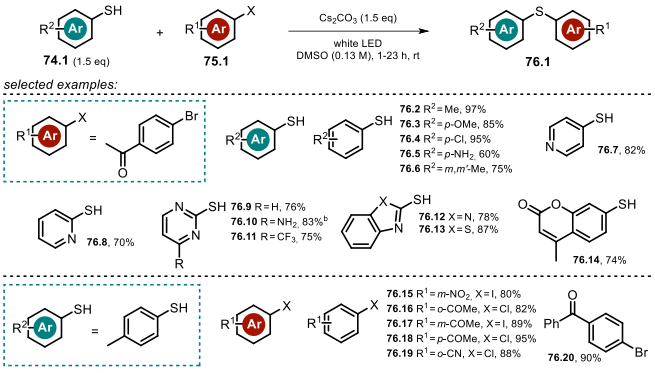

Scheme 43. Selected examples for the thiolation of aryl halides. [a]50 mmol scale; [b]Cs_2CO_3 (2 eq.).

Remarkably fast coupling reactions (1 h) were observed between electron deficient aryl halides and electron rich thiophenols. In addition, benzylic halides revealed to convert similarly. Following the developed protocol allowed for the mild and efficient late-stage functionalization of pharmaceutically active compounds.

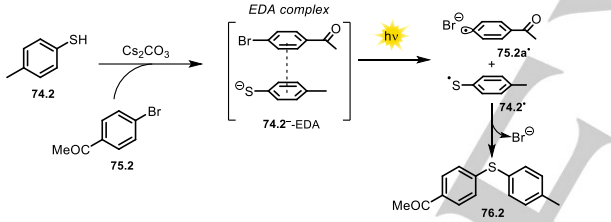

Scheme 44. Proposed reaction mechanism for the C-S cross-coupling reaction of thiophenols and aryl halides *via* the formation of a visible-light-absorbing EDA complex.

The formation of an EDA complex **74.2**$^-$-EDA between thiophenolate **74.2**$^-$ and aryl halide **75.2** was confirmed by UV-vis spectroscopy and TD-DFT calculations. The arising charge-transfer absorption band allows to initiate the reaction with visible light *via* an electron transfer from the thiolate anion to the aryl halide, followed by cleavage of the halide anion. The formed thiyl- and aryl radical combine to afford the C−S cross-coupled product **76.2** (Scheme 44).

Based on the perfluoroalkylation of alkenes and alkynes, it was recently shown that the anionic counterpart involved in the EDA complex formation can be utilized catalytically.[129] In presence of base, 2-bromophenol (**BrPhOH**) was found to promote the visible-light-mediated 1,2-addition of fluoroalkyl iodides to alkenes and alkynes. Noteworthy, although a significant amount of product was formed in the reaction of allylbenzene **77.2** and ethyl iododifluoroacetate **56.6** in absence of phenol catalyst, the yield could be doubled using a catalytic amount of **BrPhOH**. The use of a more polar solvent gave rise to Heck-type coupling products. Allylphenols, acting themselves as catalyst, could be converted to either the addition product **79.1** or the coupling product **80.1** without adding **BrPHOH**.

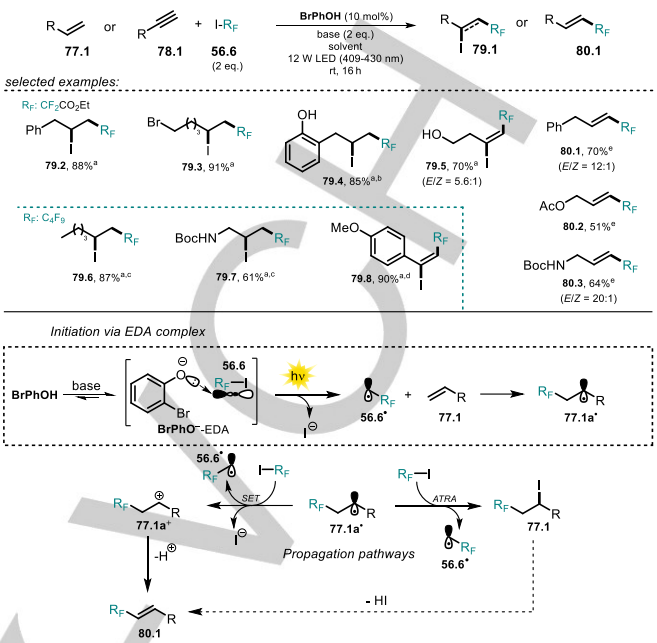

Scheme 45. Selected examples for fluoroalkylation of alkenes and alkynes affording addition products or Heck-type coupling products (top) [a]Using KOAc (2 eq) in DCE; [b]without **BrPhOH** in dioxane; [c]Cs_2CO_3 instead of KOAc; [d]K_2CO_3 instead of KOAc; [e]Using K_2CO_3 (2 eq.) in DMSO; Proposed reaction mechanism for the visible-light-promoted fluoroalkylation using 2-bromophenol as catalyst (bottom).

Initiation of the reaction is proposed to occur *via* EDA complex formation between phenolate **BrPhO**$^-$ and alkylating reagent **56.6**. The photoexcited EDA complex causes the formation of radical **56.6**$^\bullet$ which reacts with the olefin **77.1** to yield the radical intermediate **77.1a**$^\bullet$. Depending on the reaction medium, either abstraction of an iodine atom from **56.6** affords the addition product **79.1** or SET with **56.6** gives rise to the cationic intermediate **77.1a**$^+$, which forms the Heck-type product **80.1** upon deprotonation (Scheme 45).

3.7. Organic Anions promoting the Radical-Nucleophilic Substitution ($S_{RN}1$) Reaction

In the course of $S_{RN}1$ reactions, radicals and radical anions are formed as intermediates and chain mechanisms are likely to occur. Proposed for the first time in the 1960s,[130,131] the reaction affords nucleophilic substitution on aromatic and aliphatic compounds and tolerates a wide scope of nucleophiles and substrates.[132] Initiation is commonly achieved by photoinduced electron transfer from an electron-rich anionic nucleophile to an electron-poor acceptor, leading to the open-shell nucleophile Nu$^\bullet$ and a radical anion. EDA complex formations between nucleophile and substrate are reported and allow to initiate $S_{RN}1$ reactions by using less-energetic light.[125] Upon mesolytic bond cleavage, the resulting radical R$^\bullet$ is trapped by the nucleophile and forms a radical anion. A single electron transfer from the radical anion [R-Nu]$^{\bullet-}$ to the acceptor R-X affords the desired substitution product along with another radical anion [R-X]$^{\bullet-}$, which enables the propagation of a chain reaction (Scheme 46), provided that this SET is thermodynamically favourable.

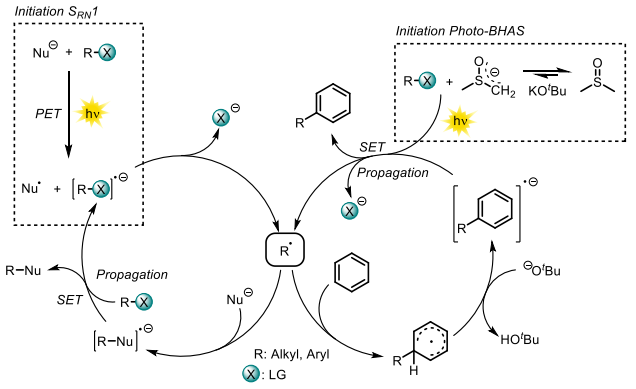

Scheme 46. General reaction mechanism for the radical-nucleophilic substitution ($S_{RN}1$) reaction and for the photoinitiated base-promoted homolytic aromatic substitution reaction (photo-BHAS).

Closely related to the concept of the light-induced $S_{RN}1$ reaction is the photoinitiated base-promoted homolytic aromatic substitution reaction (photo-BHAS), affording C−H arylated products starting from aryl or alkyl halides in presence of a strong base (*e.g.* KO^{t}Bu or NaH). The reactive intermediate R$^\bullet$ is proposed to add to the arene forming an aromatic radical, which is converted into the respective radical anion by deprotonation and eventually gives the arylated product upon SET to propagate the chain reaction. In absence of further additives, it has recently been shown that the dimsyl anion can be excited by visible light and plays a pivotal role for initiating the reaction (see Scheme 46).[133] The initiation of the BHAS reaction was also reported by other photo-activation modes *e.g.* through PET from an iridium sensitizer to R-X, or upon light-excitation of an *in-situ* formed photosensitive complex between KO^{t}Bu and phenanthroline.[134,135] Non-nucleophilic bases are commonly employed to avoid the competing $S_{RN}1$ reaction pathway. Light-mediated substitutions following the $S_{RN}1$ reaction with organic anions as nucleophiles have been studied extensively and were subject of recent reviews[4,132,136–140] and thus will not be further discussed herein.

3.8. Direct Photodecarboxylation of Carboxylates

In presence of light, various organic carboxylates are known to undergo photodecarboxylation (PDC) affording CO_2 and either a carbanion intermediate (heterolytic cleavage) or an alkyl radical intermediate in combination with a solvated electron (homolytic cleavage). Meiggs *et al.*[141] performed flash photolysis of sodium phenyl acetate and could proof the formation of a benzyl radical intermediate by transient absorption spectroscopy. The formation of toluene, besides polyacids and bibenzyl, may suggest a competing heterolytic bond cleavage mechanism. Reaction pathways *via* high-energetic carbanion or radical intermediates are favoured in compounds bearing stabilizing substituents. Hence, PDC is often observed upon irradiation of dissociated aryl acetic acids **81.1**, causing intermediates which benefit from benzylic stabilization (Scheme 47). The light-mediated decomposition of carboxylates has been covered in detail in various reviews and thus is beyond the scope of this work.[142–144]

Photobases are important initiators of photopolymerization processes. Xanthone and thioxanthone acetic acids (**81.7-8**) form carbanions upon decarboxylation and have recently received interest as amine free alternatives to enable efficient thiol-epoxy polymerization.[145,146]

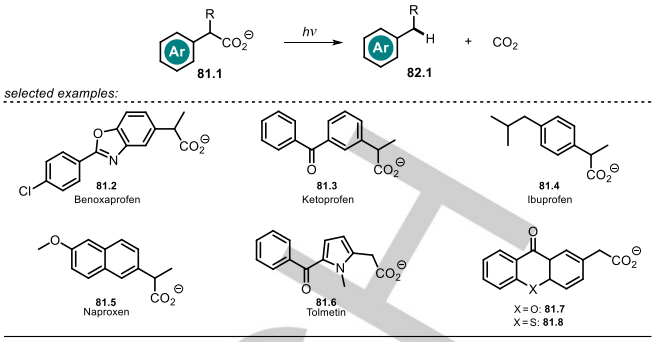

Scheme 47. General scheme for the photodecarboxylation of dissociated aryl acetic acids and prominent examples.

3.9. Sulfite Anions used in Photoreactions

The ability of cheap and available sulfite salt to generate hydrated electrons upon irradiation renders its use attractive (Scheme 48). The method was successfully applied for the photodegradation of hazardous halogenated pollutants like monochloroacetic acid[147] **83** and perfluorooctanesulfonate[148] . However, harmful high-energetic UV-light (254 nm) is necessary to photoexcite sulfite anions and the process efficiency suffers in more complex media due to light attenuation by scattering or competing absorption of other organic compounds including the solvent.

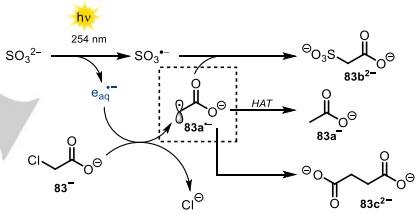

Scheme 48. Dechlorination of monochloroacetic acid by solvated electrons produced upon UV-light excitation of sulfite anions.

4. Summary and Outlook

Organic anions and light are a perfect combination to achieve challenging synthetic transformations as either reagents or photocatalysts. Compared to a corresponding neutral molecule, the absorption spectrum of the negatively charged anion usually exhibits a bathochromic shift and often fluorescence is exclusively observed for the anionic species. This allows photochemical conversions with less-energetic light, in many cases visible light. Fluorescence quenching studies enable the verification of interactions between substrates and the excited chromophore. The seminal work of Soumillion and co-workers in this field and their excellent review[33] demonstrated early the potential of organic anions as strong photoreductants in the dechlorination of arenes and the desulfonylation of sulfonamides using excited 2-naphtholate. The oxygen-centered radicals of photoexcited anionic decatungstates allow to break strong C(sp^3)−H bonds of non-prefunctionalized alkanes to form new carbon bonds. Synergistic approaches of HAT and transition-metal-catalysis have recently found widespread interest and also enabled asymmetric reactions. In addition to the use of anions as photocatalysts, excited anions found applications as strong reductants to activate a reaction partner *via* PET followed by a subsequent conversion of both open-shell intermediates. Examples are the arylation of azaallylanions or the Heck-type

arylation of vinylphenols. Photoexcited organic anions allow cyclization reactions yielding pyrazoles or participate in ring-expanding reactions. Moreover, organic anions serve as potent electron-rich donor molecules for the formation of light-absorbing EDA complexes.

Overall, the use of photoexcited anions harbours enormous potential for applications in synthetic organic chemistry. We observe an increasing research interest in applying photoexcited anions as catalysts or reagents and hope that this review will stimulate more contributions to this yet underexplored but emerging field, which holds promise for many more exciting applications in organic synthesis.

Matthias Schmalzbauer completed his M.Sc. in chemistry at the University of Regensburg (Germany) in 2016. During his master studies, he joined the group of Prof. König and spent a research period at the UNC (Córdoba, Argentina) under the supervision of Prof. Roberto A. Rossi. He received his Ph.D. from the University of Regensburg in 2020 and is currently a postdoctoral fellow in the König group with research interests focussing on organic photoredox catalysis.

Michela Marcon got her master's degree in Chemistry in 2019 at University of Padova (Italy), under the supervision of Dr. Xavier Companyó. She then joined the group of Prof. König as an Erasmus trainee, working on the photocatalytic generation of carbanions. Currently, she is PhD student in the König group.

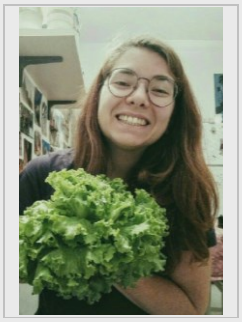

Burkhard König received his Ph.D. from the University of Hamburg and continued his scientific education as a postdoctoral fellow with Prof. M. A. Bennett, Australian National University, Canberra, and Prof. B. M. Trost, Stanford University. Since 1999 he is a full professor of organic chemistry at the University of Regensburg. His current research interests are synthetic methods in organic synthesis utilizing visible light and applications of photochromic molecules.

Acknowledgements

This work was supported by the German Science Foundation (DFG, KO 1537/18-1) and has received funding from the European Research Council (ERC) under the European Union's Horizon 2020 Research and Innovation Programme (grant agreement No. 741623).

Conflict of Interest

The authors declare no conflict of interest.

Keywords: Excited anion • photoredox catalysis • photoreductant • synthetic photochemistry • single electron transfer

[1] M. A. Fox, *Chem. Rev.* **1979**, *79*, 253–273.
[2] L. M. Tolbert, *Acc. Chem. Res.* **1986**, *19*, 268–273.
[3] E. Krogh, P. Wan, *Top. Curr. Chem.* **1990**, *156*, 93-116.
[4] J.-P. Soumillion, *Top. Curr. Chem.* **1993**, *168*, 93–141.
[5] T. O. Baldwin, *Structure* **1996**, *4*, 223–228.
[6] K. J. Hellingwerf, J. Hendriks, T. Gensch, *J. Phys. Chem. A* **2003**, *107*, 1082–1094.
[7] S. Faraji, A. Dreuw, *Annu. Rev. Phys. Chem.* **2014**, *65*, 275–292.
[8] W. Lee, G. Kodali, R. J. Stanley, S. Matsika, *Chem. Eur. J.* **2016**, *22*, 11371–11381.
[9] A. H. Zimmerman, R. Gygax, J. I. Brauman, *J. Am. Chem. Soc.* **1978**, *100*, 5595–5597.
[10] J. P. Soumillion, P. Vandereecken, M. Van Der Auweraer, F. C. De Schryver, A. Schanck, *J. Am. Chem. Soc.* **1989**, *111*, 2217–2225.
[11] N. Tamaoki, Y. Takahashi, T. Yamaoka, *J. Chem. Soc. Chem. Commun.* **1994**, 1749–1750.
[12] J. Smid, *Angew. Chem. Int. Ed.* **1972**, *11*, 112–127.
[13] M. J. Kaufman, S. Gronert, D. A. Bors, A. Streitwieser, *J. Am. Chem. Soc.* **1987**, *109*, 602–603.
[14] Y. Marcus, G. Hefter, *Chem. Rev.* **2006**, *106*, 4585–4621.
[15] H. D. Roth, *Top. Curr. Chem.* **1990**, *156*, 1–19.
[16] D. Rehm, A. Weller, *Isr. J. Chem.* **1970**, *8*, 259–271.
[17] N. A. Romero, D. A. Nicewicz, *Chem. Rev.* **2016**, *116*, 10075–10166.
[18] B. Legros, P. Vandereecken, J. P. Soumillion, *J. Phys. Chem.* **1991**, *95*, 4752–4761.
[19] E. Vander Donckt, J. Nasielski, P. Thiry, *J. Chem. Soc. D* **1969**, 1249–1250.
[20] C. Kerzig, M. Goez, *Phys. Chem. Chem. Phys.* **2015**, *17*, 13829–13836.
[21] M. Brautzsch, C. Kerzig, M. Goez, *Green Chem.* **2016**, *18*, 4761–4771.
[22] M. Schmalzbauer, I. Ghosh, B. König, *Faraday Discuss.* **2019**, *215*, 364–378.
[23] X. F. Zhang, I. Zhang, L. Liu, *Photochem. Photobiol.* **2010**, *86*, 492–498.
[24] K. Hashimoto, T. Kawai, T. Sakata, *Chem. Lett.* **1983**, *12*, 709–712.
[25] E. F. Zwicker, L. I. Grossweiner, *J. Phys. Chem.* **1963**, *67*, 549–555.
[26] L. I. Grossweiner, E. F. Zwicker, *J. Chem. Phys.* **1961**, *34*, 1411–1417.
[27] K. Kimura, T. Miwa, M. Imamura, *Chem. Commun.* **1968**, 1619–1621.
[28] A. Aguirre-Soto, K. Kaastrup, S. Kim, K. Ugo-Beke, H. D. Sikes, *ACS Catal.* **2018**, *8*, 6394–6400.
[29] C. Munkholm, D. R. Parkinson, D. R. Walt, *J. Am. Chem. Soc.* **1990**, *112*, 2608–2612.
[30] A. Joshi-Pangu, F. Lévesque, H. G. Roth, S. F. Oliver, L. C. Campeau, D. Nicewicz, D. A. DiRocco, *J. Org. Chem.* **2016**, *81*, 7244–7249.
[31] E. Speckmeier, T. G. Fischer, K. Zeitler, *J. Am. Chem. Soc.* **2018**, *140*, 15353–15365.
[32] F. Speck, D. Rombach, H. A. Wagenknecht, *Beilstein J. Org. Chem.* **2019**, *15*, 52–59.
[33] C. K. Prier, D. A. Rankic, D. W. C. MacMillan, *Chem. Rev.* **2013**, *113*, 5322–5363.
[34] C. Streb, *Dalton Trans.* **2012**, *41*, 1651–1659.
[35] I. Ghosh, J. Khamrai, A. Savateev, N. Shlapakov, M. Antonietti, B.

König, *Science* **2019**, *365*, 360–366.
[36] Y. Y. Loh, K. Nagao, A. J. Hoover, D. Hesk, N. R. Rivera, S. L. Colletti, I. W. Davies, D. W. C. MacMillan, *Science* **2017**, *358*, 1182–1187.
[37] I. Ghosh, T. Ghosh, J. I. Bardagi, B. König, *Science* **2014**, *346*, 725–728.
[38] I. Ghosh, B. König, *Angew. Chem. Int. Ed.* **2016**, *55*, 7676–7679.
[39] J. I. Bardagi, I. Ghosh, M. Schmalzbauer, T. Ghosh, B. König, *Eur. J. Org. Chem.* **2018**, *2018*, 34–40.
[40] M. Neumeier, D. Sampedro, M. Májek, V. A. de la Peña O'Shea, A. Jacobi von Wangelin, R. Pérez-Ruiz, *Chem. Eur. J.* **2018**, *24*, 105–108.
[41] M. Majek, A. Jacobi Von Wangelin, *Acc. Chem. Res.* **2016**, *49*, 2316–2327.
[42] I. Ghosh, L. Marzo, A. Das, R. Shaikh, B. König, *Acc. Chem. Res.* **2016**, *49*, 1566–1577.
[43] I. Ghosh, *Phys. Sci. Rev.* **2019**, *4*, 20170185, DOI: 10.1515/psr-2017-0185.
[44] C. S. Wang, P. H. Dixneuf, J. F. Soulé, *Chem. Rev.* **2018**, *118*, 7532–7585.
[45] J. P. Cole, D.-F. Chen, M. Kudisch, R. M. Pearson, C.-H. Lim, G. M. Miyake, *J. Am. Chem. Soc.* **2020**, *142*, 13573–13581.
[46] J. A. Christensen, B. T. Phelan, S. Chaudhuri, A. Acharya, V. S. Batista, M. R. Wasielewski, *J. Am. Chem. Soc.* **2018**, *140*, 5290–5299.
[47] D. Weir, J. C. Scaiano, *Chem. Phys. Lett.* **1986**, *128*, 156–159.
[48] A. Samanta, K. Bhattacharyya, P. K. Das, P. V. Kamat, D. Weir, G. L. Hug, *J. Phys. Chem.* **1989**, *93*, 3651–3656.
[49] J. C. Scaiano, M. Tanner, D. Weir, *J. Am. Chem. Soc.* **1985**, *107*, 4396–4403.
[50] L. J. Johnston, *Chem. Rev.* **1993**, *93*, 251–266.
[51] B. R. Arnold, J. C. Scaiano, W. G. McGimpsey, *J. Am. Chem. Soc.* **1992**, *114*, 9978–9982.
[52] I. A. MacKenzie, L. Wang, N. P. R. Onuska, O. F. Williams, K. Begam, A. M. Moran, B. D. Dunietz, D. A. Nicewicz, *Nature* **2020**, *580*, 76–80.
[53] D. Gosztola, M. P. Niemczyk, W. Svec, A. S. Lukas, M. R. Wasielewski, *J. Phys. Chem. A* **2000**, *104*, 6545–6551.
[54] J. Haimerl, I. Ghosh, B. König, J. Vogelsang, J. M. Lupton, *Chem. Sci.* **2019**, *10*, 681–687.
[55] S. Fukuzumi, K. Ohkubo, T. Suenobu, *Acc. Chem. Res.* **2014**, *47*, 1455–1464.
[56] T. Hering, T. Slanina, A. Hancock, U. Wille, B. König, *Chem. Commun.* **2015**, *51*, 6568–6571.
[57] B. Zilate, C. Fischer, C. Sparr, *Chem. Commun.* **2020**, *56*, 1767–1775.
[58] K. A. Margrey, D. A. Nicewicz, *Acc. Chem. Res.* **2016**, *49*, 1997–2006.
[59] Q. Xu, B. Zheng, X. Zhou, L. Pan, Q. Liu, Y. Li, *Org. Lett.* **2020**, *22*, 1692–1697.
[60] P. D. Morse, T. M. Nguyen, C. L. Cruz, D. A. Nicewicz, *Tetrahedron* **2018**, *74*, 3266–3272.
[61] E. Alfonzo, F. S. Alfonso, A. B. Beeler, *Org. Lett.* **2017**, *19*, 2989–2992.
[62] K. Wang, L. G. Meng, L. Wang, *Org. Lett.* **2017**, *19*, 1958–1961.
[63] K. Tu, T. Xu, L. Zhang, Z. Cheng, X. Zhu, *RSC Adv.* **2017**, *7*, 24040–24045.
[64] T. Krappitz, K. Jovic, F. Feist, H. Frisch, V. P. Rigoglioso, J. P. Blinco, A. J. Boydston, C. Barner-Kowollik, *J. Am. Chem. Soc.* **2019**, *141*, 16605–16609.
[65] J. Li, Z. Liu, S. Wu, Y. Chen, *Org. Lett.* **2019**, *21*, 2077–2080.
[66] P. D. Morse, D. A. Nicewicz, *Chem. Sci.* **2015**, *6*, 270–274.
[67] H. T. Qin, S. W. Wu, J. L. Liu, F. Liu, *Chem. Commun.* **2017**, *53*, 1696–1699.
[68] M. Majek, F. Filace, A. J. Von Wangelin, *Beilstein J. Org. Chem.* **2014**, *10*, 981–989.
[69] D. P. Haria, B. König, *Chem. Commun.* **2014**, *50*, 6688–6699.
[70] V. Srivastava, P. P. Singh, *RSC Adv.* **2017**, *7*, 31377–31392.
[71] K. Liang, Q. Liu, L. Shen, X. Li, D. Wei, L. Zheng, C. Xia, *Chem. Sci.* **2020**, *11*, 6996–7002.
[72] J. P. Soumillion, P. Vandereecken, F. C. De Schryver, *Tetrahedron Lett.* **1989**, *30*, 697–700.
[73] M. Ayadim, J. P. Soumillion, *Tetrahedron Lett.* **1996**, *37*, 381–384.
[74] A. H. Dwivedi, U. Pande, *J. Photochem. Photobiol. A* **2003**, *154*, 303–309.
[75] J. F. Art, J. P. Kestemont, J. P. Soumillion, *Tetrahedron Lett.* **1991**, *32*, 1425–1428.
[76] E. Hasegawa, N. Izumiya, T. Miura, T. Ikoma, H. Iwamoto, S. Y. Takizawa, S. Murata, *J. Org. Chem.* **2018**, *83*, 3921–3927.
[77] E. Hasegawa, Y. Nagakura, N. Izumiya, K. Matsumoto, T. Tanaka, T. Miura, T. Ikoma, H. Iwamoto, K. Wakamatsu, *J. Org. Chem.* **2018**, *83*, 10813–10825.
[78] E. Hasegawa, T. Tanaka, N. Izumiya, T. Kiuchi, Y. Ooe, H. Iwamoto, S. Y. Takizawa, S. Murata, *J. Org. Chem.* **2020**, *85*, 4344–4353.
[79] J. H. Baxendale, *Radiation Res. Suppl.* **1964**, *4*, 114–138.
[80] E. J. Hart, *Surv. Prog. Chem.* **1969**, *5*, 129-184.
[81] G. V. Buxton, C. L. Greenstock, W. P. Helman, A. B. Ross, *J. Phys. Chem. Ref. Data* **1988**, *17*, 513–886.
[82] D. Zhu, L. Zhang, R. E. Ruther, R. J. Hamers, *Nat. Mater.* **2013**, *12*, 836–841.
[83] L. Zhang, D. Zhu, G. M. Nathanson, R. J. Hamers, *Angew. Chem. Int. Ed.* **2014**, *53*, 9746–9750.
[84] I. Ghosh, R. S. Shaikh, B. König, *Angew. Chem. Int. Ed.* **2017**, *56*, 8544–8549.
[85] M. Schmalzbauer, T. D. Svejstrup, F. Fricke, P. Brandt, M. J. Johansson, G. Bergonzini, B. König, *Chem* **2020**, doi.org/10.1016/j.chempr.2020.08.022.
[86] S. Mahboobi, S. Dove, A. Sellmer, M. Winkler, E. Eichhorn, H. Pongratz, T. Ciossek, T. Baer, T. Maier, T. Beckers, *J. Med. Chem.* **2009**, *52*, 2265–2279.
[87] H. Liu, H. Tang, D. Yang, Q. Ji, *Chinese J. Pharm.* **2011**, *42*, 641–644.
[88] M. Raghu, J. Grover, S. S. V. Ramasastry, *Chem. Eur. J.* **2016**, *22*, 18316–18321.
[89] E. Lamy, L. Nadjo, J. M. Saveant, *J. Electroanal. Chem.* **1977**, *78*, 403–407.
[90] M. K. Nazeeruddin, R. Humphry-Baker, D. Berner, S. Rivier, L. Zuppiroli, M. Graetzel, *J. Am. Chem. Soc.* **2003**, *125*, 8790–8797.
[91] A. Ionescu, E. I. Szerb, Y. J. Yadav, A. M. Talarico, M. Ghedini, N. Godbert, *Dalton Trans.* **2014**, *43*, 784–789.
[92] S. Y. Takizawa, R. Kano, N. Ikuta, S. Murata, *Dalton Trans.* **2018**, *47*, 11041–11046.
[93] C. Kerzig, X. Guo, O. S. Wenger, *J. Am. Chem. Soc.* **2019**, *141*, 2122–2127.
[94] H. Yin, Y. Jin, J. E. Hertzog, K. C. Mullane, P. J. Carroll, B. C. Manor, J. M. Anna, E. J. Schelter, *J. Am. Chem. Soc.* **2016**, *138*, 16266–16273.
[95] Potential is reported *vs*. the Fc^+/Fc couple and was converted against SCE by adding +380 mV (see ref.[96]).
[96] V. V. Pavlishchuk, A. W. Addison, *Inorganica Chim. Acta* **2000**, *298*, 97–102.
[97] L. L. Costanzo, S. Pistarà, G. Condorelli, *J. Photochem.* **1983**, *21*, 45–51.
[98] Y. Qiao, Q. Yang, E. J. Schelter, *Angew. Chem. Int. Ed.* **2018**, *57*, 10999–11003.
[99] V. De Waele, O. Poizat, M. Fagnoni, A. Bagno, D. Ravelli, *ACS Catal.* **2016**, *6*, 7174–7182.

[100] D. Ravelli, M. Fagnoni, T. Fukuyama, T. Nishikawa, I. Ryu, *ACS Catal.* **2018**, *8*, 701–713.

[101] K. Suzuki, N. Mizuno, K. Yamaguchi, *ACS Catal.* **2018**, *8*, 10809–10825.

[102] C. Tanielian, *Coord. Chem. Rev.* **1998**, *178–180*, 1165–1181.

[103] N. Li, J. Liu, B. Dong, Y. Lan, *Angew. Chem. Int. Ed.* **2020**, doi.org/10.1002/anie.202008054

[104] D. Ravelli, M. Fagnoni, T. Fukuyama, T. Nishikawa, I. Ryu, *ACS Catal.* **2018**, *8*, 701–713.

[105] I. B. Perry, T. F. Brewer, P. J. Sarver, D. M. Schultz, D. A. DiRocco, D. W. C. MacMillan, *Nature* **2018**, *560*, 70–75.

[106] P. J. Sarver, V. Bacauanu, D. M. Schultz, D. A. DiRocco, Y. hong Lam, E. C. Sherer, D. W. C. MacMillan, *Nat. Chem.* **2020**, *12*, 459–467.

[107] H. Cao, Y. Kuang, X. Shi, K. L. Wong, B. B. Tan, J. M. C. Kwan, X. Liu, J. Wu, *Nat. Commun.* **2020**, *11*, 1–8.

[108] Z. Y. Dai, Z. S. Nong, P. S. Wang, *ACS Catal.* **2020**, *10*, 4786–4790.

[109] P. Fan, C. Zhang, L. Zhang, C. Wang, *Org. Lett.* **2020**, *22*, 3875–3878.

[110] L. Wang, T. Wang, G. J. Cheng, X. Li, J. J. Wei, B. Guo, C. Zheng, G. Chen, C. Ran, C. Zheng, *ACS Catal.* **2020**, *10*, 7543–7551.

[111] Y. Kuang, H. Cao, H. Tang, J. Chew, W. Chen, X. Shi, J. Wu, *Chem. Sci.* **2020**, *11*, 8912–8918.

[112] K. Liang, T. Li, N. Li, Y. Zhang, L. Shen, Z. Ma, C. Xia, *Chem. Sci.* **2020**, *11*, 2130–2135.

[113] G. Filippini, M. Nappi, P. Melchiorre, *Tetrahedron* **2015**, *71*, 4535–4542.

[114] Q. Wang, M. Poznik, M. Li, P. J. Walsh, J. J. Chruma, *Adv. Synth. Catal.* **2018**, *360*, 2854–2868.

[115] M. Li, S. Berritt, L. Matuszewski, G. Deng, A. Pascual-Escudero, G. B. Panetti, M. Poznik, X. Yang, J. J. Chruma, P. J. Walsh, *J. Am. Chem. Soc.* **2017**, *139*, 16327–16333.

[116] T. Zhang, Y. Meng, J. Lu, Y. Yang, G.-Q. Li, C. Zhu, *Adv. Synth. Catal.* **2018**, *360*, 3063–3068.

[117] R. S. Suarez, R. G. Segura, *Tetrahedron Lett.* **1988**, *29*, 1071–1074.

[118] C. Sánchez-Sánchez, E. Pérez-Inestrosa, R. García-Segura, R. Suau, *Tetrahedron* **2002**, *58*, 7267–7274.

[119] Y. R. Luo, *Comprehensive Handbook of Chemical Bond Energies*, CRC Press, **2007**.

[120] K. Maruyama, Y. Kubo, *J. Org. Chem.* **1985**, *50*, 1426–1435.

[121] R. Suau, C. Sánchez-Sánchez, R. García-Segura, E. Pérez-Inestrosa, *Eur. J. Org. Chem.* **2002**, 1903–1911.

[122] F. N. Figueroa, A. A. Heredia, A. B. Peñéñory, D. Sampedro, J. E. Argüello, G. Oksdath-Mansilla, *J. Org. Chem.* **2019**, *84*, 3871–3880.

[123] A. K. Ganguly, S. S. Alluri, D. Caroccia, D. Biswas, C. H. Wang, E. Kang, Y. Zhang, A. T. McPhail, S. S. Carroll, C. Burlein, et al., *J. Med. Chem.* **2011**, *54*, 7176–7183.

[124] D. K. Rayabarapu, A. Zhou, K. O. Jeon, T. Samarakoon, A. Rolfe, H. Siddiqui, P. R. Hanson, *Tetrahedron* **2009**, *65*, 3180–3188.

[125] C. G. S. Lima, T. D. M. Lima, M. Duarte, I. D. Jurberg, M. W. Paixão, *ACS Catal.* **2016**, *6*, 1389–1407.

[126] G. E. M. Crisenza, D. Mazzarella, P. Melchiorre, *J. Am. Chem. Soc.* **2020**, *142*, 5461–5476.

[127] M. Nappi, G. Bergonzini, P. Melchiorre, *Angew. Chem. Int. Ed.* **2014**, *53*, 4921–4925.

[128] B. Liu, C. H. Lim, G. M. Miyake, *J. Am. Chem. Soc.* **2017**, *139*, 13616–13619.

[129] E. Zhu, X. X. Liu, A. J. Wang, T. Mao, L. Zhao, X. Zhang, C. Y. He, *Chem. Commun.* **2019**, *55*, 12259–12262.

[130] N. Komblum, R. E. Michel, R. C. Kerber, *J. Am. Chem. Soc.* **1966**, *88*, 5662–5663.

[131] G. A. Russell, W. C. Danen, *J. Am. Chem. Soc.* **1966**, *88*, 5663–5665.

[132] R. A. Rossi, A. B. Pierini, A. B. Peñéñory, *Chem. Rev.* **2003**, *103*, 71–167.

[133] M. E. Budén, J. I. Bardagí, M. Puiatti, R. A. Rossi, *J. Org. Chem.* **2017**, *82*, 8325–8333.

[134] Y. Cheng, X. Gu, P. Li, *Org. Lett.* **2013**, *15*, 2664–2667.

[135] Z. Xu, L. Gao, L. Wang, M. Gong, W. Wang, R. Yuan, *ACS Catal.* **2015**, *5*, 45–50.

[136] R. A. Rossi, J. F. Guastavino, M. E. Budén, in *Arene Chemistry: Reactions Mechanisms and Methods for Aromatic Compounds* (Ed.: J. Mortier), John Wiley & Sons, Inc., New Jersey, **2015**, pp. 243–268.

[137] J. I. Bardagí, M. E. Budén, R. A. Rossi, *Targets Heterocycl. Syst.* **2016**, *20*, 247–282.

[138] M. E. Budén, S. E. Martín, R. A. Rossi, in *CRC Handbook of Organic Photochemistry and Photobiology* (Eds.: A. Griesbeck, M. Oelgemöller, F. Ghetti), CRC Press, Boca Raton, **2012**, pp. 347–368.

[139] A. B. Peñéñory, J. E. Argüello, in *Handb. Synth. Photochem.* (Eds.: A. Albini, M. Fagnoni), Wiley-VCH Verlag GmbH & Co. KGaA, Weinheim, **2010**, pp. 319–351.

[140] A. Studer, D. P. Curran, *Nat. Chem.* **2014**, *6*, 765–773.

[141] T. O. Meiggs, L. I. Grossweiner, S. I. Miller, *J. Am. Chem. Soc.* **1972**, *94*, 7981–7986.

[142] D. Budac, P. Wan, *J. Photochem. Photobiol. A* **1992**, *67*, 135–166.

[143] F. Boscá, M. L. Marín, M. A. Miranda, in *CRC Handbook of Organic Photochemistry and Photobiology Second Ed.*. (Eds.: W. Horspool, F. Lenci), CRC Press, **2003**, pp. 64 1–10.

[144] M. Lukeman, in *CRC Handbook of Organic Photochemistry and Photobiology Third Ed.* (Eds.: A. Griesbeck, M. Oelgemöller, F. Ghetti), CRC Press, **2012**, pp. 715–726.

[145] J. A. Blake, E. Gagnon, M. Lukeman, J. C. Scaiano, *Org. Lett.* **2006**, *8*, 1057–1060.

[146] X. Dong, P. Hu, G. Zhu, Z. Li, R. Liu, X. Liu, *RSC Adv.* **2015**, *5*, 53342–53348.

[147] X. Li, J. Ma, G. Liu, J. Fang, S. Yue, Y. Guan, L. Chen, X. Liu, *Environ. Sci. Technol.* **2012**, *46*, 7342–7349.

[148] Y. Gu, W. Dong, C. Luo, T. Liu, *Environ. Sci. Technol.* **2016**, *50*, 10554–10561.

10.1002/ange.202009288

Entry for the Table of Contents

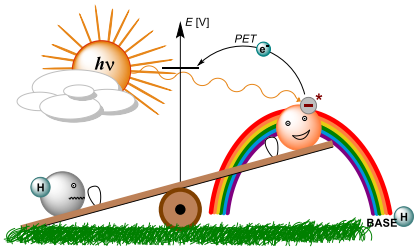

I'm so excited! Anions act as powerful single electron reductants from their photoexcited state in catalytic or stochiometric transformations and are easily activated in the presence of a base. Their absorption is shifted bathochromically compared to the neutral molecules and visible light is often sufficient for their excitation.

Twitter: @ChemistryKoenig